Indian J. Phys. **76B** (2), 107–138 (2002)

REVIEW

I J P B
an international journal

Atmospheric ozone depletion and its effect on environment

S K Midya*
Centre for Space Physics, 114/V/1A Raja S. C. Mullick Road, Kolkata-700 047, West Bengal, India
and
P K Jana
Department of Chemistry, Howrah Zilla School, Howrah-711 101, West Bengal, India
E-mail : skmidya@hotmail.com

Received 10 November 2000, accepted 20 December 2001

Abstract : A critical review on ozone depletion since 1928 is presented Various types of works on O_3 depletion and its effects on environment are performed by different investigators throughout the world. In this review, we have presented up-to-date information on O_3 depletion.

Keywords : O_3 depletion, UV-radiation.

PACS Nos. : 94.10.Fa, 94.10.Rk.

Plan of the Article

1. Introduction

O_3 is a minor constituent of the atmosphere. It is mainly distributed in the stratosphere. Maximum concentration of O_3 occurs around 25 km altitude.

Farman *et al* [1] first reported the dramatic decrease of ozone concentration at Antarctica. Afterwards, it was verified by different investigators throughout the world. It is also observed that O_3 concentration decreases gradually with smaller amount in the other parts of the world except Antarctica. Different theories have been proposed by different investigators. In this paper, we have presented the chemistry of O_3 depletion in detail. The effects of ozone depletion on our environment are also presented.

esponding Author
ess for Communication : Department of Physics, Serampore College, Serampore, Hooghly-712 201, West Bengal, India

2. Measurement of atmospheric ozone

There are several methods and instruments used to measure the total ozone content and its profile with altitude generally in Dobson Unit (DU), which is one thousandth of a centimeter or in ozone partial pressure or in ozone mixing ratio. Ground-based observations use two bands of solar UV radiations—one almost unaffected by ozone and the other strongly absorbed by ozone. Measurement of the ratio of intensities of these two bands allows one to calculate the amount of ozone through which the sunlight has been transmitted. Satellite-borne instrument records backscatter on reflected solar UV radiations. Solar Backscattered UV Instrument (SBUV) and Total Ozone Mapping Spectrometer (TOMS) are at work aboard nimbus-7 satellites, SBUV provides information of both total ozone and its distribution with altitude. The total ozone over the entire globe is mapped on a daily basis. The recent measurements, detection and observation of ozone with different instruments at different stations throughout the world are briefly discussed in this section.

Observations by balloon-borne experiment and Dobson spectrometer were taken at Dakshin Gangotri, Antarctica during 1988-89. It is reported that in September-October, 1988, ozone depletions were much less pronounced than those occurred during a similar period in 1987 [2]. The meteorological techniques, the profile and Bowen ratio techniques and eddy correlation techniques are used to determine the flux of ozone in a Maize crop throughout the growing season of it in 1987. It is observed that the profile technique underestimates the fluxes of O_3 by 40%. The fluxes of O_3 determined by the modified Bowen ratio technique and eddy-correlation technique were nearly the same [3]. Measurement of O_3 concentrations at various heights above and below the canopy of a mature slash pine forest 18 km northest of Gainsville, Florida showed that the O_3 concentration near the ground were significantly different from those obtained in and around the canopy [4]. Surface O_3 measurements at Bandung, west Java, Indonesia for the period December 1986 - December 1988 showed the significant diurnal maximum (35 ppbv) occurring at noon, minimum (3.5 ppbv) at night and diurnal average is 17.5 ppbv. Maximum O_3 concentrations occur earlier in wet month (March) than in dry month (July) [5]. Dobson spectrophotometric total ozone, Umkehr and ECC ozonesonde O_3 vertical distribution were observed in Boulder, Colorado, in April 1990 when similar observations were made quasi-simultaneously with a ground based NOAA SEUV-2, SN-2, satellite O_3 instrument at the Ball corporation research and manufacturing facility in Boulder. Data obtained from Ball corporations and NASA was used to assess laboratory calibrations of the SBUV-2 instrument [6]. A ground based high power differential absorption lidar system was used to measure stratospheric ozone concentration profiles from 20-25 km altitude. It is located at an elevation of 2300 m in the San Gabriel Mountains, Southern California, since January 1988. It is compared with SAGE II satellite data [7]. The GOMOS (global O_3 monitor by occulation of stars) instrument comprises of a telescope feeding 2 spectrographs, mounted on a dedicated steerable platform. The emmittance of the atmosphere 250-675 nm can be measured by comparing the spectrum of a star outside the atmosphere and through it. The tangential column of O_3 is determined by its UV and Chappais band absorption [8]. It has been observed from both the SAGE (stratospheric Aerosol and Gas Experiment) and ozonesonde measurement that there is a reduction in O_3 of ~0.5% per year upto 1989 at mid-latitudes of Northern Hemisphere [9]. At the 2 finish EMAP background stations of Ahtari (forested site) and Uto (an offshore island) ozone measurements showed that the mean O_3 levels were relatively high, with maximum monthly values of 41 and 42 ppb, respectively that occurred in April at both sites nearly irrespective of wind direction pointing to a global feature. Surface uptake is an important sink in the local O_3 budget especially during late spring, summer and early autumn. Chemical losses are more efficient in the winter when the ground is covered by snow [10]. The nitric oxide/ozone chemiluminescence technique was used to measure the reactive NO/NOY species by the NASA high altitude AR-2 aircraft and the destruction of O_3 through catalytic cycles by reactive Cl species is described [11]. Chemiluminescence of the ozone reaction with Coumarin 47 absorbed on silica-gel was used to measure the stratospheric and tropospheric ozone concentrations [12]. Diurnal and seasonal variations of ozone were shown in a suburban area of Valladolid, Spain from May 1988 to 1989. It is reported that diurnal variations are affected by temperature and solar radiations NO and NO_2 precursors affected ozone concentrations in air [13].

A cryogenic Fourier transform spectrometer (F.T.S.) developed for limb emission measurements in the mid IR-region from balloon-borne platforms is a rapid scanning interferometer using a modified Michelson arrangement achieving a spectral resolution of 0.04/cm. The trace gases CO_2, H_2O, O_3, CH_4, N_2O, HNO_3, N_2O_5, $ClONO_2$, CF_2Cl_2, $CFCl_3$, CHF_2Cl, CCl_4 and C_2H_6 were identified in the measured spectra. These gases are important in the O_3 chemistry and/or climate [14]. From the field study of surface exchange of NOx over grass on Halvergate Marshes in the U.K. the measurement of vertical concentration profiles of NO, NO_2 and O_3, the measurement of momentum,

heat and O_3 fluxes by eddy correlation, it was reported that NO_2 concentration decreased with height due to surface uptake and simultaneous gas phase chemical reactions. Under night time conditions with low O_3 concentrations, the influence of chemical reactions on O_3 fluxes was important [15]. In the rural south-western United states, O_3 concentrations above 100 ppb were regularly observed. It was reported that the maximum O_3 concentration occurred in the Summer and the minimum in the Winter. It was concluded that if stratospheric O_3 have a significant influence on the high O_3 days, it should be easily detected in the Spring. Ozone photochemically produced in urban areas is transported to the sites by the prevailing winds. The Los Angeles Basin is the major contributor to the O_3 episodes in the rural areas of the South Western United States [16]. The development of the Improved Limb Atmosphere Spectrometer (ILAS) for measuring the O_3 concentration vertical profiles from the advanced Earth observing satellite is discussed. It includes a MOS linear sensor and uses the sun as a light source. Limb Atmosphere IR Spectrometer (LAS) comprises of a solar-occulation limb sensor, an IR sensor and a multichannel spectroscopic sensor. It was used to measure the stratospheric O_3 concentrations in the low latitude northern hemisphere in April 1984. It was reported that the total column O_3 is less over the Pacific Ocean and it is maximum at a longitude of 90° [17]. ECC ozonesonde measurements of the vertical distribution of O_3 and air temperature at Point Barrow, Alaska during January 16 – April 19, 1989 showed that out of 33 sounding made, 17 measured total O_3 amounts of 400-531 DU, 13 measured 350-399 DU total O_3 and 1 measured 304 DU total O_3. Two sounding did not attain high enough altitudes for estimations of total O_3. But total O_3 amounts in winter and spring in Antarctica in recent years have ranged 125-275 DU. Stratospheric air temperatures over Point Barrow were never colder than –70°C and were often as warm as –50°C [18]. The Cryogenic Limb Array Etalon Spectrometer (CLAES), a instrument of the NASA, Upper Atmosphere Research Satellite (UARS) is used to measure stratospheric altitude profiles of temperature, pressure, concentrations of O_3, H_2O, CH_4, N_2O, NO, NO_2, N_2O_5, HNO_3, $ClONO_2$, HCl, CFC-11 and CFC-12 since 1991 [19].

The NASA airborne differential absorption lider (DIAL) system is used to measure the large-scale variation of O_3 and aerosols in the summer arctic troposphere [20]. Vertical O_3 profile measurements with balloon-borne sensors in the Arctic during January and February, 1990 showed the repeated minima in the 22 km region suggesting chemical ozone depletion [21]. Vertical ozone distributions above Pretoria, South Africa measured by Dobson Spectrophotometer are presented from 1965-68. The variability of O_3 at different altitude is discussed [22]. A spectroscopic method used for determination of atmospheric ozone using Indigo disulfonate solution is discussed [23]. Fifteen vertical ozone profiles measurements on sunny windless days in August, 1990 between 430 m and 2200 m above the sea level on the mountain Kanin in Slovenia, showed an increase of O_3 concentrations from the morning to the evening. The influence of a cold frost, a valley wind system and local wind are also shown [24]. The observations of total O_3 at Tromsoe (Northern Norway), Sodan-kyla (Northern Finland) and Murmausk (North western soviet union) for 1987-89, comparisons of the total O_3 with stratospheric temperatures at Sodankyla (1965-1988) showed no severe O_3 depletion, the spring variability O_3 in the lower stratosphere due to meteorological variability, two maximum of lower tropospheric O_3, one in the Spring due to large scale photochemical causes and the other in Summer due to the emissions of hydrocarbons and NOx in Europe [25].

TOMS satellite column ozone data in latitudes 70°s–70°N from November 1978 to May 1990 showed the trends in O_3 as a function of latitude, longitude and month. The trends are highly seasonal and dependent on location. Near the equator, the monthly trends are not significantly different from zero. For high latitudes, most of the estimated monthly trends are negative. In January, February and March, there are some positive trend estimations in the western Hemisphere around latitude 60°N. A large depletion develops during the Spring (September to November) in the southern high latitude region [26]. Airborne and spaceborne experiments were conducted in Amazones, Brazil in September 1989 to measure O_3, CO_2, CO, CH_4 and particulate matter from biomass from an aircraft. Fires were observed from satellite imagery and the smoke optical thickness, particle-size and profiles of the extinction coefficient were measured using sunphotometers in the aircraft and from the ground. It was reported that there was a strong relation between the spatial distribution of fires and O_3 concentrations, between biomass burning and concentrations of trace gases, particulate matter and O_3. It will suggest a correlation between biomass burning in the tropics and O_3 formation [27]. The chemical balloon-borne devices developed for direct measurements of O_3 in the atmosphere may be divided into electrochemical and chemiluminescent groups. The operating principle of the former is based on the reaction of O_3 with a KI solution. Iodine released by this reaction is quantitatively measured by a coulometric method. These electrochemical instruments have widely been adopted for measuring atmospheric O_3 and the data employed for various applications are derived chiefly from two types of ozonesonde. The Brewer Mast

(BM) Bubbler and the electrochemical concentration cell (ECC) [28]. An airborne differential absorption lidar (DIAL) used during the 1991 Lake Michigan Ozone study to map the vertical distribution of O_3 concentrations across Lake Michigan down wind of urban and industrial areas of the south lake region is compared with air borne *in-situ* O_3 measurements [29].

Ozone measurement using the NOAA instrumental King Air research aircraft over Lake Michigan during the Summers of 1990 and 1991 showed that the increased O_3 was accompanied by moderately increased SO_2 and NOx. The elevated O_3 concentrations were related to emissions from the urban region located near the southern and south western shores of Lake Michigan. Total ozone concentration was measured by the Dobson Spectrophotometer 40 at Uccle (50°48'N, 4°21'E), Belgium for the period 1971-1986 [30]. The satellite Spectrometer BUFS-2 for measurement of total ozone and vertical ozone distribution was described. It comprises of a double monochromator with spherical 600 ruling/mm diffraction gratings with a focal distance of 250 mm and 8.2 degree by 8.2 degree field of view. The spectral channels are switched by adjusting the intermediate slits realized by a disk with openings which are derived by a step-by-step motor. The total measurement time for all channels is ~20 s and the spectral half width is ~1 nm [31]. A star pointing UV-visible spectrometer has the capability to measure reactive gases in the O_3 layer *e.g.* O_3, NO_2, NO_3 and ClO_2 using the sun as a source of light. The instrument was deployed at Abisko in northern Sweden during the 1991-1992 European Arctic Stratospheric Ozone Expedition [32].

The improved stratospheric and mesospheric sounder (ISMAS), a limb-viewing IR radiometer, an instrument on the NASA upper atmospheric Research satellite launched in September 1991 enables daily mapping over much of the earth's temperature, concentrations of 8 chemical species (H_2O-vap, CH_4, O_3, HNO_3, NO_2, NO, N_2O_5 and CO) and aerosol opacity in the stratosphere and mesosphere. It was 8 separate focal planes, each consisting of a 4 element detector array instrument with a movable mirror to scan the limb in elevation and to view may be to either side of the space craft to improve geographical coverage [33]. Measurements of the atmosphere backscattered UV albedo used from satellites for >20 yrs to measure O_3, the largest continuous record from the solar back scattered UV instrument (SBUM) and total O_3 mapping spectrometer (TOMS) on the Nimbus 7 satellite, since November 1978 showed no significant trends near the equator, but significant trends larger than predicted by homogeneous chemistry at mid to high latitudes in both hemispheres [34]. DOAS (Differential optical absorption spectrometry) measurements of NO_3, NO_2 and O_3 were performed on the atmospheric of the French Atlantic coast in June 1989. The differential absorption spectroscopy technique associated with a Fourier transform spectrometer was used to measure SO_2, NO_2, HCHO, and O_3 concentrations at the urban site of the campus of the free University of Brussels, Belgium since October, 1990. It consists of a source (either a high pressure xenon lamp or a tungsten filament) and a 800-m-long path system. The spectra are recorded in the 26000–38000 cm^{-1} [35].

The scanning radiometer (SR) NOAA satellites during the 1970s included a visible channel that overlapped closely to the chappuis absorption band of O_3 ~600 nm. The Antarctic atmosphere and surface contain no other significant absorbers of radiation at those wave lengths, which makes Antarctica an ideal region to isolate the O_3 signal in the visible channel data. So SR data may be used to map Antarctic O_3 prior to 1978, since accurate detailed maps of total O_3 were not available before the launch of the total O_3 mapping spectrometer (TOMS) in late 1978 [36] Measurements of surface ozone for the period November 17 to January 11, 1993 in Tromsoe, Norway, using American and Russiuan type ozonometers gave almost identical results It was reported that there was no diurnal variation probably due to the lack of sunlight during the polar night and O_3 decreased normally during day time through reactions with pollutants such as NOx and hydrocarbons [37]. Surface O_3 measurements performed by chemiluminescence ozonometer at various sites of industrial and residential areas and in the suburbs as well during polar winter period showed weak diurnal variation and the background O_3 level is 15–25 ppb [38]. The UV-photometer uses radioluminescence source (RLS) with very high long-term temporal emission stability instead of generally used unstable Hg-1 amp. The RLS emission power is 3×10^{11} quantum/sec. It is used to measure the ozone concentration by selective absorption of UV-radiation by O_3 molecule [39]. Total O_3 measurements at Uccle (50°48'N, 4°21'E) with Dobson spectrophotometer 40 since August, 1971 and with Brewer instrument from 16th July, 1983, the reduced thickness of SO_2 as calculated from measurements with Brewer spectrophotometer and *in situ* measurements of SO_2 near the ground in the urban area of Brussels showed a decreasing trend of SO_2. It is reported that SO_2 decrease at Uccle has introduced a fictitious Dobson total O_3 trend that amounts to mean value of −1.47% per decade [40]. Measurement of ClO, O_3, H_3O, temperature and pressure by the Microwave limb Sounder (MLS) launched on 12th September, 1991 on the upper atmosphere research Satellite (UARS) reveals that chlorine in the lower stratosphere was almost completely converted to chemically reactive

forms in both northern and southern polar winter vortices. It occurred in the south long before the development of the Antarctic ozone hole [41]. Measurements of O_3 and aerosol distributions with an airborne lidar system in the low land and boreal forest regions of eastern Canada during July–August, 1990, showed that over 33% of the troposphere (0–12 km) along the flight track at latitudes from about 45 to 50° N had significantly enhanced O_3 due to stratospheric intrusions and in the middle to upper troposphere, the extent of the enhanced O_3 generally exceeded 40% [42]. The SAGE II (1985-1989) and SBUV-version 6 (1979-1986) global ozone vertical structure satellite data sets to determine the long term trends in ozone as a function of altitude (pressure) and latitude were studied. SAGE II data only available during the period of increasing solar activity, showed an increase in ozone with time in the upper stratosphere attributed largely to rising solar activity. Study of combined SBUV and SAGE II data over the 11-years solar cycle showed a clear response of ozone to 11-years solar variations and allowed a decoupling of solar effects, quasi-biennial oscillations (QBO) and trends [43].

The central Equatorial pacific Experiment and Balloon-borne soundings at Solomon Islands (9°24'S, 160°6'E) and Christmas Islands (2°N, 157°30'W) and satellite measurements showed the volume mixing ratios of ozone frequently well below 10 nanomoles per mole both in the marine boundary layer (MBL) and between 10 km and the tropopouse [44]. Satellite observation with the Middle Atmosphere High Resolution Spectrograph Investigation (MAHRSI) showed a sharp peak in OH density at an altitude of 65–70 km, thus consistent with observations from Halogen Occulation Experiment (HALOE) on the NASA Upper Atmosphere Research Satellite (UARS) which showed an unexplained H_2O layer at the same level. It was reported from stratopause OH measurements and O_3 observation from cryogenic Infrared Spectrometers and Telescopes for the Atmosphere (CRISTA) experiment that the catalytic loss of O_3 due to odd Hydrogen chemistry is less than that predicted. So the dominant portion of the ozone deficit problem in standard model is a consequence of over estimation of the OH density in the upper stratosphere and mesosphere [45]. Observations of total ozone by Dobson spectrophotometer at Poleward of 60°S in midwinter, the satellite-borne Total Ozone Mapping Spectrometer in June and/or July at 65°S, the satellite borne Tiros Operational Vertical Sounder (TOVS) over the Central Antarctic Plateau in Winter, the satellite borne microwave Limb Sounder (MLS) were made and compared. Measurements of total ozone at Faraday, Antarctica (65°S) by a ground based visible spectrometer of the design system d'Analyse per observations zenithales (SAOZ) showed a winter maximum [46]. Balloon-borne measurements of total reactive nitrogen, NOy [= NOx(NO + NO_3) + HNO_3 + $ClONO_2$ + $2N_3O_5$ + HO_2NO_2] recorded by MIPAS-B instrument in the Arctic vortex on February 11, 1995 indicate 50% deficit of NOy between 16 and 22 km by particle sedimentation suggested that denitrification was caused predominantly by nitric acid trihydrate (NAT) in small number densities. It was reported that this denitrification is responsible for increase in arctic ozone loss [47].

3. Observation of ozone depletion

In general, ozone is depleted everywhere, year to year, season to season and day to day. Some important observations of ozone depletion are mentioned below.

Investigators	*Information obtained*
Farman *et al* [1] (1985)	first reported that the dramatic decrease of O_3 concentration occurs during Spring at Antarctic observed at British Antarctic Survey Station, Halley Bay (76°S, 27°W) during 1957-84 (Figure 1) and monthly mean October values is decreased by 30–40% since 1977.

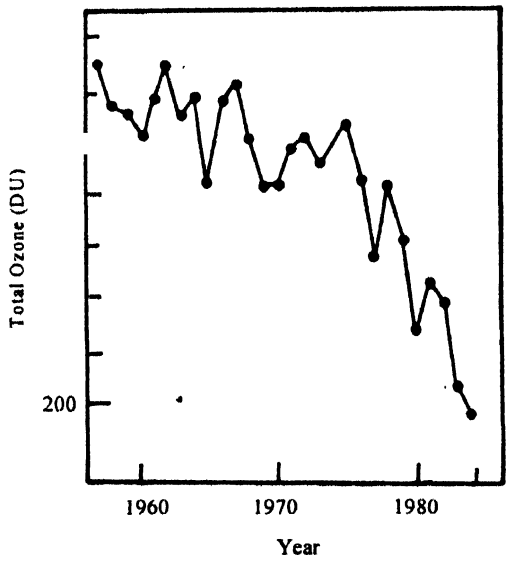

Figure 1. Spring time ozone variation during 1957–84 at Halley Bay (76°S, 27°W), a British Antarctic Survey Station

Hofmann *et al* [48] (1986)	showed that the total ozone declined by 35% whereas the integrated ozone between 14 and 18 km by 70% and within the polar vortex by 90%.
Schoeberl and Kruger [49] (1986)	reported dramatic year to year decline in total ozone over Antarctic Spring.

CH_3 will react with NO leading to O_3 production as follows [44, 70 and 71].

$$RO_2 + NO \rightarrow OH + NO_2 \ (R = H),$$

$$NO_2 + h\nu \rightarrow NO + O \ (\lambda < 420 \text{ nm}),$$

$$O + O_2 + M \rightarrow O_3 + M.$$

HO_2 is formed by the following reaction as reported by Crutzen [71] :

$$CO + OH \rightarrow H + CO_2,$$

$$H + O_2 + M \rightarrow HO_2 + M.$$

Both HO_2 and peroxy radical, CH_3O_2 are formed during the oxidation of methane.

Attri *et al* [72] discovered a surprising source of ozone which is generated in spontaneous bursts even in the absence of sunlight and nitrogen oxides —namely, the exuberant mass of colour emitting sparklers that are lit during the Diwali festivities, which take place every year during October and November in Delhi, India. Sparklers depend on a combination of salts of metals to originate their colour and sparkle —these include potassium perchlorate, sodium oxalate, calomel, aluminium and manganese when burnt, a significant amount of radiation emitted by these constituents having a wavelength below 240 nm is sufficient to dissociate atmospheric molecular oxygen into atomic oxygen, enabling the reaction $O_2 + O \rightarrow O_3$ to take place. Slanger *et al* [73] suggests that the photolysis of vibrationally excited oxygen can provide an extra source of ozone.

$$O_3 + h\nu \rightarrow O\ (^3p) + O_2\ (X^3\Sigma g),$$

$$O_2^*\ (X^3\Sigma g) + h\nu \rightarrow O_2\ (B^3\Sigma\bar{U}) \rightarrow 2O,$$

$$3O + 3O_2 \rightarrow 3O_3.$$

The above mechanism becomes very important when vibration levels ($v'' > 15$) are populated. According to the theory of nuclear symmetry, the rate of ozone formation [74] from collisions of O and isotopically homonuclear O_2 depends on whether the O_2 molecule is in an *f* (allowed) or an *e* (restricted) parity level state. Approximately, 78 percent of the restricted O_2 (*e*) levels produces O_3 with the same efficiency as the allowed O_2 (*f*) levels and this theory explains the special enhanced formation of the completely asymmetric isotopomer $^{16}O^{17}O^{18}O$. Symmetry-induced kinetic isotope effects (SIKIES) analysis can be applied to the first step of the Chapman mechanism [68] for ozone formation.

$$O_2(^3\Sigma\bar{g}) + O(^3p_j) \xrightarrow{Ka} O_3^*,$$

$$O_3^* \xrightarrow{k_d} O_2(^3\Sigma\bar{g}) + O(^3p_j),$$

$$O_3^* \xrightarrow{Ks,\ M} O_3(^1A_1),$$

where, O_3^* is a collision complex and *Ka*, k_d and *Ks* are the phenomenological association, dissociation and stabilization rate constants, respectively. O_2 and O_3 are in their ground electronic states and the O atom can be in either its ground ($^3p_2$) or first two excited ($^3p_1$, $^3p_0$) spin orbit states.

The unusually high enrichment in most of the heavy isotopomers of ozone [76] has been observed in tropospheric [75,77], and stratospheric ozone [78] and has been studied in detail in numerous laboratory experiments [79–81]. The isotope composition of atmospheric ozone is [^{16}O] = 99.756%, [^{17}O] = 0.038% and [^{18}O] = 0.205% through out the troposphere and stratosphere. The following channels of ozone formation are considered and specific rate coefficients are measured and derived [82] shown in Table 1 relative to the standard rate [83] for $^{16}O + {}^{32}O_2 + M$ of 6.05×10^{-34} cm $^6S^{-1}$.

Table 1. Measured and derived rate co-efficients for ozone formation processes.

Isotope mass	Enrichment mass spectrometric (%)	Measured rate coefficient		Derived rate coefficient	
		Reaction	Value	Reaction	Value
48	0 0	$^{16}O+{}^{16}O\ {}^{16}O$	1 00	—	—
49	11.3	$^{17}O+{}^{16}O\ {}^{16}O$	1.03	$^{16}O+{}^{17}O\ {}^{16}O$	1.17
50	13 0	$^{18}O+{}^{16}O\ {}^{16}O$	0.93	$^{16}O+{}^{18}O\ {}^{16}O$	1.27
50	12 1	$^{16}O+{}^{17}O\ {}^{17}O$	1.23	$^{17}O+{}^{16}O\ {}^{17}O$	1.11
51	–1.8	$^{17}O+{}^{17}O\ {}^{17}O$	—	$^{17}O+{}^{17}O\ {}^{17}O$	1.02
52	14.4	$^{16}O+{}^{18}O\ {}^{18}O$	1.53	$^{18}O+{}^{16}O\ {}^{18}O$	1.01
52	9.5	$^{18}O+{}^{17}O\ {}^{17}O$	1.03	$^{17}O+{}^{18}O\ {}^{17}O$	1.21
53	8.3	$^{17}O+{}^{18}O\ {}^{18}O$	1 31	$^{18}O+{}^{17}O\ {}^{18}O$	1.09
54	–4.6	$^{18}O+{}^{18}O\ {}^{18}O$	1.03	—	—

Thiemens [84] reported that the formation of asymmetric ozone species ($^{16}O\ {}^{16}O\ {}^{18}O$ and $^{16}O\ {}^{16}O\ {}^{17}O$) is favoured because it can proceed through a greater number of reactive quantum states than the formation of the symmetric isotope ($^{16}O\ {}^{16}O\ {}^{16}O$). The collision of atomic and molecular oxygen leads to the formation of a vibrationally excited O_3 transition state. The latter can either dissociate or lose or gain energy by collision to form a stable O_3 molecule. The symmetric isotope species is less likely to form a stable molecule than the asymmetric species because some vibrational-vibrational and some vibrational-rotational coupling terms are not allowed for the symmetric species. The asymmetric species can distribute energy better and is more likely to couple to the exit channel that leads to a stable molecule. There is no mass dependency but rather a subtle symmetry factor that produces the anomalous ozone.

Sulphur dioxide injected into the atmosphere catalyses mid stratospheric ozone production [85] as follows :

$$SO_2 + h\nu \rightarrow SO + O \ (\lambda < 220 \text{ nm}),$$

$$SO + O_2 \rightarrow SO_2 + O,$$

$$2(O + O_2 + M \rightarrow O_3 + M).$$

$$\text{Net} : 3O_2 \rightarrow 2O_3.$$

4.2. Depletion of atmospheric ozone :

Ozone is also depleted by several processes. Several theories have been proposed for ozone depletion causing an ozone hole. Natural, chemical and dynamical theories are mainly important. In natural theory, solar UV-radiation, sunspot cycle related to 11-year solar cycle, volcanic eruption *etc.* and in chemical theory HOx, Ox, NOx, Cl, ClOx, Br, BrOx, SOx, CHOx, [86] and PSCs (polar stratospheric clouds) play an important role in the ozone destruction.

In dynamical theory, dynamics of the atmosphere is related to the dramatic decrease of O_3 concentration. According to this theory, O_3 is not depleted, it is redistributed in the stratosphere. As a result, O_3 hole is created at Antarctica during Spring time. Polar vortex is a small region of polar atmosphere isolated by the polar circulation during polar Winter. In south polar regions, the polar vortex is usually centered over eastern Antarctica. Antarctic polar vortex is more intense than its Arctic counterpart. Antarctic polar vortex does not break down before Spring and probably, it is related to stratospheric warming.

(i) Effect of solar UV-radiation

Ozone is depleted by absorbing solar UV-radiation. There are three types of UV-region : UV-A, UV-B and UV-C. The wavelength range between 2000–2800 Å is known as UV-C region. It is lethal to man and living organisms and totally absorbed by atmospheric ozone. The wavelength range from 2800 Å to 3200 Å is known as UV-B region. Ozone absorbs, but not all radiations and is lethal to many forms of life. UV-radiations above 3200 Å called UV-A region is relatively harmless and is absorbed only slightly by atmospheric ozone.

$$O_3 + UV \rightarrow O + O_2.$$

Since O_3 is very reactive, an ozone molecule combines with an O atom to produce two O_2 molecules

$$O + O_3 \rightarrow 2O_2.$$

Ozone may also be removed by the following reaction :

$$O_3 + O_3 \rightarrow 3O_2.$$

(ii) Volcanic eruption

Volcanic eruption causes atmospheric ozone depletion directly by the release of chlorine and indirectly by accumulation of released aerosol which provides larger area for heterogeneous reactions. Again SO_2 injected into the atmosphere due to volcanic eruption may also affect ozone by absorbing radiation. SO_2 absorbs radiation strongly between 180 and 235 nm, weekly between 260–340 nm and very weekly between 340 to 390 nm [87]. So sulphurdioxide has the potential to reduce the transmission of solar flux, reducing the photolysis rates of the key species such as O_2 and hence reduces the rate of ozone formation [56].

$$SO_2 + h\nu \rightarrow SO + O \ (\lambda < 220 \text{ nm}).$$

Sulphur photochemistry on ozone formation and depletion was supported by eruption of Mount Pinatubo in June 1991. In the first month or so after the eruption, the large amount of SO_2 injected into the tropical atmosphere catalyses mid-stratospheric ozone production [85]. After one or two months, most of the SO_2 has been oxidised to sulphate aerosols causing ozone loss. Again the SO_2 cloud absorbs solar radiation, thereby reducing the rate of O_2 photolysis and hence of ozone production.

(iii) HOx catalysed ozone depletion

The atmospheric ozone is photodissociated by solar UV-radiation producing electronically excited $O(^1D)$ atoms which can take part in the formation of OH radicals [88, 89] by the following way :

$$O_3 + h\nu \rightarrow O(^1D) + O_2 \ (\lambda \leq 320 \text{ or } 410 \text{ nm}),$$

where $h\nu$ is a photon of wavelength λ,

$$O(^1D) + H_2O \rightarrow 2OH.$$

The hydroxyl radical thus produced can react with carbon monoxide or methane to form peroxy radicals *e.g.*, HO_2. These radicals also deplete the tropospheric ozone [90] as follows :

$$HO_2 + O_3 \rightarrow OH + 2O_2.$$

(iv) Cl and ClOx catalysed ozone depletion

In 1974, Molina and Rowland [91] first suggested the following chlorine catalysed ozone depletion

$$Cl + O_3 \rightarrow ClO + O_2,$$

$$\underline{ClO + O \rightarrow Cl + O_2}$$

$$\text{Net} : O_3 + O \rightarrow O_2 + O_2.$$

Molina and Molina [92] in the year 1987 suggested that a ClO dimer is involved in the following reactions :

$$ClO + ClO + M \xrightarrow{K} (ClO)_2 + M,$$

$$(ClO)_2 + h\nu \rightarrow Cl + ClOO,$$

$$ClOO + M \rightarrow Cl + O_2 + M,$$

$$\underline{2(Cl + O_3 \rightarrow ClO + O_2),}$$

$$\text{Net} : 2O_3 \rightarrow 3O_2,$$

where $h\nu$ designates an UV-photon and M signifies a collisional chaperone, either N_2 or O_2 and K is the pressure-temperature dependent rate constant of the rate limiting step.

(v) Br and BrOx catalysed ozone depletion

Surface ozone depletion in Arctic spring was mainly due to a catalytic cycle involving the radicals Br and BrO [93].

These species are rapidly converted to the non-radical species HBr, HOBr and $BrNO_3$. McConnel [94] suggested that cycling of inorganic bromine between aerosols and the gas phase maintaining high levels of Br and BrO, destroys ozone. Fan and Daniel [95] proposed a mechanism based on aqueous phase chemistry which rapidly converts HBr, HOBr and $BrNO_3$ back to Br and BrO radicals shown in Figure 3.

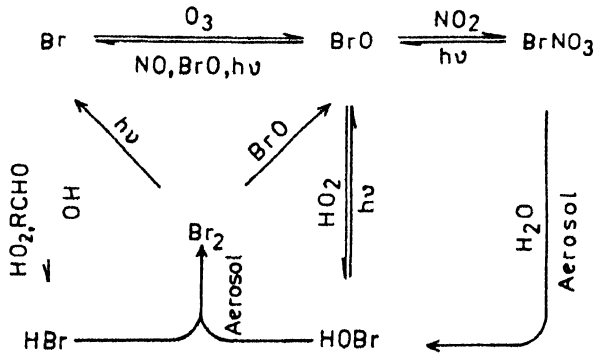

Figure 3. Chemical cycling of inorganic Br and BrO radicals catalysing ozone depletion

$BrNO_3$ is rapidly scavenged by the aerosol and hydrolysed to HOBr as follows :

$$BrNO_3(g) \xrightarrow{H_2O} HOBr(aq) + HNO_3(aq).$$

The rapid formation of Br_2 from reaction of HOBr with Br^- in acid solution is as follows [96] :

$$HOBr(aq) + Br^{\ominus} + H^{\oplus} \rightarrow Br_2(aq) + H_2O.$$

(vi) Chlorine-bromine catalysed ozone depletion

McElroy *et al* [97] suggested chlorine-bromine coupled O_3 destruction mechanism as follows :

$$\left.\begin{array}{l} ClO + BrO \rightarrow Cl + Br + O_2, \\ ClO + BrO \rightarrow Br + OClO, \\ ClO + BrO \rightarrow BrCl + O_2, \\ BrCl + h\nu \rightarrow Br + Cl, \\ Cl + O_3 \rightarrow ClO + O_2, \\ Br + O_3 \rightarrow BrO + O_2, \end{array}\right\}$$

Net : $2O_3 \rightarrow 3O_2$.

Both (IV) and (VI) mechanisms require sunlight in the near UV to visible part of the spectrum because at night, ClO recombines to form Cl_2O_2, which is not reactive towards O_3 and BrO reactants to form BrCl and $BrONO_2$. The O_3 depletion is greatest when the exposure to sunlight is longest at lower latitudes and later in the Spring [98].

(vii) Cl and HOx catalysed ozone depletion

Solomon *et al* [99] suggested Cl and OH radicals coupled ozone depletion mechanism as follows :

$$HO_2 + ClO \rightarrow HOCl + O_2,$$
$$HOCl + h\nu \rightarrow OH + Cl,$$
$$Cl + O_3 \rightarrow ClO + O_2,$$
$$OH + O_3 \rightarrow HO_2 + O_2,$$

Net : $2O_3 \rightarrow 3O_2$.

The above mechanism reveals that O atoms could not be involved quantitatively in O_3 depletion because the concentration of O atoms was too low in the polar stratosphere [100].

(viii) CO and HOx catalysed ozone depletion

In the troposphere the following reactions [50,51] are responsible for ozone depletion :

$$CO + OH \rightarrow H + CO_2,$$
$$H + O_2 + M \rightarrow HO_2 + M,$$
$$HO_2 + O_3 \rightarrow OH + 2O_2,$$

Net : $CO + O_3 \rightarrow CO_2 + O_2$.

(ix) NOx catalysed ozone depletion

NOx catalyses the destruction of stratospheric ozone as follows :

$$NO_2 + O_3 \rightarrow NO_3 + O_2,$$
$$NO_3 + NO_2 + M \rightarrow N_2O_5 + M,$$

Net : $2NO_2 + O_3 \rightarrow N_2O_5 + O_2$.

NO_3 is rapidly photolysed during daytime and N_2O_5 is mainly produced during night-time [101]. Bekki *et al* [102] reported the following ozone depletion

$$NO + O_2 \rightarrow NO_2 + O_2.$$

Johnston *et al* [103] calculated significant global ozone reduction due to NOx ($NO + NO_2$) emission from high speed civil transfer air craft flying in the stratosphere considering only homogeneous chemistry. Total O_3 removal rate in the stratosphere is determined chiefly by the HOx and halogen catalytic cycles whose relative rates are controlled by the NOx abundance [104]. Zipf and Prasad [105] reported from laboratory experiments that photo-excitation of O_2 ($B^3\Sigma u$) molecules and short lived collision complexes or weekly bound $N_2 : O_2$ dimers by the absorption of solar Schumann-Runge (SR) and Herzberg band and continuum radiation, is an efficient source of NOx ($NO + NO_2$) in the stratosphere and possibly in the troposphere by the reactions :

$$O_2 + h\nu \rightarrow O_2^*,$$
$$O_2^* + N_2 \rightarrow N_2O + O,$$
$$O_2^* + N_2 \rightarrow NO + NO,$$
$$[O_2.N_2] + h\nu \rightarrow [N_2.O_2]^*,$$
$$[O_2.N_2]^* \rightarrow NO + NO,$$

$$[O_2.N_2]^* \rightarrow N_2 + O_2,$$
$$[O_2.N_2]^* \rightarrow N_2 + O + O,$$
$$[O_2.N_2]^* \rightarrow [O_2.N_2] + h\nu.$$

(x) Polar stratospheric clouds (PSCs) and its chemistry on ozone depletion

Under normal Winter conditions in the lower stratosphere, the temperature within the polar vortex fall low enough that clouds of nitric acid trihydrate (NAT) and ice crystals can form despite the dryness of the stratosphere (2–4 ppm mixing ratio of H_2O). These clouds are known as polar stratospheric clouds (PSCs) [106]. Atmospheric recent observations show that some PSCs may be composed of $HNO_3.2H_2O$ and $HNO_3.3H_2O$. Laboratory data indicates that nucleation and persistence of metastable $HNO_3.2H_2O$ may be favoured in polar stratospheric clouds over more stable $HNO_3.3H_2O$. Vapour transfer from $HNO_3.2H_2O$ to $HNO_3.3H_2O$ could be a key step in the sedimentation of HNO_3 [107]. Thin films of $HNO_3.2H_2O$ have also been reported by Ritzhaupt and Devlin [108], Tolbert and Middlebrook [109] and Koehler [110]. PSCs are now recognized as the key species in the Spring time destruction of ozone and the formation of ozone hole [97,99,111–13] and the sites for a group of heterogeneous reactions perturbing the normal gas phase chemistry in the polar region. The following several processes are responsible for PSC induced O_3 depletion [100].

I. Pure ice clouds (Type II) can form at temperature dropping to or below 195 K and 50 mb pressure at roughly 20 km altitude and clouds of NAT (Type I) can form at temperature 10° warmer.

II. Hydrochloric acid dissolves in ice particles along the grain boundaries.

III. The heterogeneous conversion on particles of PSCs [106,114,115] of inorganic chlorine from its less-reactive components HCl and chlorine nitrate $ClONO_2$ to Cl_2 and HOCl are believed to occur on surfaces of both type I NAT and Type II (Water ice) PSC particles when sufficient amounts of HNO_3 and H_2O condense on sulphate aerosol particles [106,114,115]. The principal reactions are as follows [116–120] :

$$HCl + ClONO_2 \xrightarrow{\text{Type I, II PSCs}} Cl_2 + HNO_3,$$
$$ClONO_2 + H_2O \xrightarrow{\text{Type II PSCs}} HOCl + HNO_3,$$
$$HOCl + HCl \xrightarrow{\text{Type I, II PSCs}} Cl_2 + H_2O.$$

IV. Atomic chlorine is then formed by the photolysis of molecular chlorine.

$$Cl_2 + h\nu \rightarrow Cl + Cl.$$

V. Atomic chlorine thus formed, initiates the catalytic chain of ozone depletion.

How PSCs and sunlight can alter the abundances of trace gases and O_3 in the polar vortex is shown by Brune *et al* [98] in Figure 4. The dotted lines indicate the available chlorine, reactive nitrogen and initial O_3. The solid lines indicate reactive chlorine ($ClO + Cl_2O_2$), HNO_3 and O_3. Ozone is rapidly depleted by reactive chlorine after all available

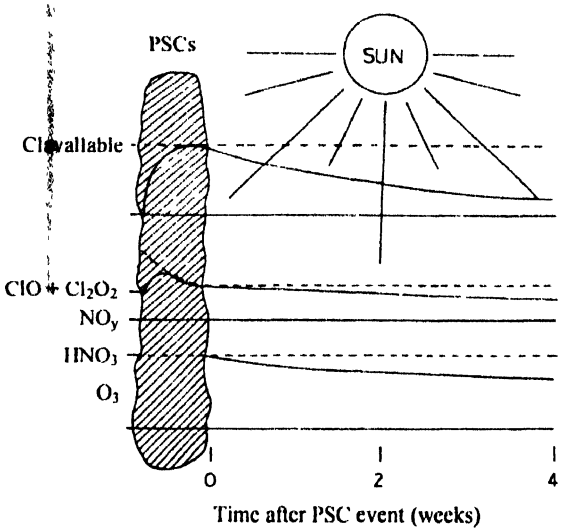

Figure 4. Variations of the abundances of trace gases by PSCs and sunlight.

chlorine becomes reactive chlorine ($ClO + Cl_2O_2$) by heterogeneous reaction on PSCs. NOy is reduced by de-nitrification of NOy by heterogeneous reactions when the PSCs evaporate, HNO_3 again becomes gaseous and is slowly photolysed to NO_2 which reduces reactive chlorine. The conversion of chlorine takes hours to days, reactive nitrogen days to weeks for denitrification and weeks for gas phase photochemistry.

5. Ozone studies over India

Ozone studies over India have already been done by different investigators at different stations. Total Ozone in India was first measured [121] at Kodaikanal (10°N, 77°E) during 1928-29, then at Bombay (19°N, 72.9°E) and Poona (18°N, 73.6°E) the National Ozone centre for India and the Regional ozone centre for the Regional Association II (Asia) of the world Meteorological Organization by Chiplonkar [122], during 1936-38, using the same photographic instrument. The India Meteorological Department (IMD) Poona first used the Dobson ozone spectrophotometer for regular measurements of ozone during 1940. Daily observations were made [123] at New Delhi (29°N, 77°E) during 1945–47, at Simla (31°N, 78°E), Poona (18°N, 73.6°E) and Kodaikanal (10°N, 77°E) during 1948-49, followed by the systematic measurement by Ramanathan at Ahmedabad (23°N, 72.6°E) in 1951, then at three more stations, Kodaikanal (10°N, 77°E), Srinagar (34°N, 74°E)

and New Delhi (29°N, 77°E) in the late fifties using Umkehr technique (124–132).

Dobson and Chiplonkar's measurements showed the existence of low values of total ozone over the tropics with little variation throughout the year and no correlation between ozone and the weather. Ramanathan and his associates showed the main features of the horizontal and vertical distribution of ozone over the tropics. The day to day variations in ozone concentrations were small. The level of maximum ozone is higher (25–28 km) in the tropics than at higher latitudes with no change of vertical distribution with seasons [124,125]. They studied the vertical distribution of atmospheric ozone on a global scale [126], the important relationship between atmospheric ozone and the general circulation of the atmosphere [127], the behavior and transport of ozone, the mean meridional distribution of ozone in different seasons, the probable transport mechanisms [128,129] and the pronounced longitudinal difference in ozone in late Winter and Spring. The Spring rise in ozone in high and middle latitudes was associated with the break-up and warming of the polar stratospheric vortex [131].

The first Indian balloon-borne electrochemical ozonesonde was introduced [133,134] in 1962, the first surface ozone recorder [135] in 1970, regular ozone sounding since 1971 and surface ozone measurements [123] since 1973. The regular total ozone measurements and vertical ozone distribution using Dobson ozone spectrophotometers were carried out at Srinagar (34°N, 74°E), New Delhi (29°N, 77°E), Mount Abu (24°N, 72°E), Ahmedabad (23°N, 72.6°E), Pune (18°N, 73.6°E), Varanasi (25.5°N, 85°E), Kodaikanal (10°N, 77°E) and Trivandrum (8.25°N, 76.9°E); regular surface ozone measurements using electrochemical sensors at Srinagar (34°N, 74°E), New Delhi (29°N, 77°E), Pune (18°N, 73.6°E), Nagpur (21°09'N, 79°09'E) Kodaikanal (10°N, 77°E) and Trivandrum (8.25°N, 76.9°E); vertical profile measurements using electrochemical balloon-borne ozonesondes at New Delhi (29°N, 77°E), Pune (18°N, 78.6°E) and Trivandrum (8.25°N, 76.9°E) stations [123].

Surface ozone in the tropics was measured by Ramanathan at Ahemadabad using Ehmert's apparatus [127] in 1954. The rocket-borne multi-channel UV-photometer ozonesonde was introduced in 1976 at the Physical Research Laboratory (PRL), Ahmedabad using the absorption of solar UV-radiation in the wavelength bands 250, 280 and 310 nm. Flown on centause and M-100 rockets, a number of ozone profiles had been obtained over Thumba (8.25°N, 76.9°E) [136–140]. High altitude balloon measurements using a suntracking multichannel radiometer of better altitude radiation than rocket-sonde were carried out [139,140] upto 35 km at Hyderabad [17.5°N, 78.6°E). At PRL, 1.27 μm photometer was used to determine the ozone concentration in 50–90 km region.

Vivekanand and Arora [141] obtained vertical profiles of ozone over Bangalore (13°N, 77.5°E) from measurements of the emission spectra of ozone in the mm-wave region using microwave radiometer operating at 110–836 GHz. Indian Middle Atmosphere Programme (IMAP) during 1982-86, its continuation IMAP-C [142], Programme involving ground based rocket and satellite systems, a two-channel rocket-borne solar UV-photometer flown from Thumba [143] and an infrared laser heterodyne system (LHS) using 9–11 μm window at NPL had been developed [144] to investigate ozone layer and other trace gases, particularly at lower latitude. Surface ozone over the Indian Ocean had also been measured [2,145,146].

A number of balloon ascents using cryogenic air samplers and PRL's multichannel sun-tracking photometers had been carried out at Hyderabad (17.5°N, 78.6°E) by PRL in collaboration with the Max Planck Institute for Aeronomy (MPAE), west Germany to measure the trace gases with ozone in the atmosphere [139,140,147,148]. Diurnal and seasonal variation of O_3, NO_2 and SO_2 during 1989 at Varanasi (25.5°N, 83°E) [149] show that maximum NO_2 and SO_2 concentrations occurred during Winter and maximum O_3 concentration during Summer. NO_2 and SO_2 peaked in the morning and evening but peak O_3 concentrations occurred in the afternoon generally between noon and 4 PM. Ozone concentration was measured in urban environment of Delhi at ground level and at hight 23, 51, 117 and 153 mts at 4 sites during 1989-90. Ozone build up was observed all over Delhi, which showed significant vertical variation of O_3 concentration. At a particular time, O_3 levels were lowest at ground level and invariably increased with increasing distance from ground [150,151]. The solar UV-B radiation at the central wave lengths 290, 300 and 310 nm was observed by a solar UV-B radiation monitoring system using UV-interference filters and a phototube mounted on a suntracker. The 310 channel data was used to derive total ozone concentration at Trivandrum (8.25°N, 76.9°E) and it was compared with that obtained at Kodaikanal (10°N, 77°E) using Dobson Spectrophotometer [152]. Measurement of solar UV-B radiation of 290–320 nm at ground level for 8 years since 1981 at the National Physical Laboratory (NPL), New Delhi, India shows a systematic anti-correlation with total atmospheric O_3 for clear days [152]. Srivastava *et al* [152], Kumar *et al* [153] and Mani [123] had also presented short-period observations and tried to correlate with UV-radiation. Chakrabarty and Peshin [154] studied the variation of O_3 concentration over Indian region after eruption of Mount Pinatubo in June, 1991. They suggested that

heterogeneous reactions do not play significant role to reduce total ozone after volcanic eruption in the low latitude region. Besides these, they also observed from ozonesonde observations at Pune (18.3°N, 73.6°E) and balloon measurement of aerosol profile at Hyderabad (17.5°N, 78.6°E) that the altitude of ozone peak is about 5 km higher than the altitude of the aerosol peak. Chakrabarty *et al* [155] concluded that long-term total ozone observations during 23–45 years by Dobson spectrophotometer at Kodaikanal (10°, 79°E), Mount Abu (24°N, 72°E), New Delhi (28°N, 77°E) and Srinagar (34°N, 74°E) show an increasing trend with the rates of 1.98, 2.33, 1.85 and 0.68% per decade respectively, no trend at Pune (18°N, 74°E), but 1.02% decrease per decade at Varanasi (25°N, 82°E). The Nimbus 7 total ozone mapping spectrometer data and Dobson data at Kodaikanal, Pune, Mt. Abu, New Delhi and Srinagar for the period November, 1978 to April, 1993 and at Varanasi for the period November, 1978 to December, 1987 are compared. These two data agree fairly well at all places except at Kodaikanal and Ahmedabad. Tropospheric and stratospheric ozone column obtained by ozonesonde at Pune for the period January, 1988 to July, 1997 and at New Delhi for March, 1989 to September, 1997 show that the variations of tropospheric and stratospheric columns are in opposite phase. At New Delhi, increase of tropospheric ozone and decrease in stratospheric ozone cause a slight decrease of total ozone column. Tropospheric marginal decrease of ozone and no change in stratospheric ozone cause almost no trend in total ozone column at Pune. The cause of the above trends can be attributed, partly to the trends of tropospheric ozone.

Jana *et al* [156] reported that the ozone concentrations occur maximum during the months of May-June and minimum during the month of December over India. In case of the station, Halley Bay (a British Antarctic Survey Station), maximum ozone concentration occurs during the months of January-February and minimum during the months of September-October. Ozone concentration gradually increases from the month of January, attains its maximum for the period of May and June, then gradually decreases and attains its minimum value for the month of December over India. But for Halley Bay, maximum ozone concentration occurs during the months of January and February, then gradually decreases, attains minimum for the month of September to October, then gradually increases. Analysis reveals an ozone trend at Trivandrum, Hyderabad, Bombay and Dumdum by –0.51, –0.02, –0.38 and –0.68% per year respectively. No trend is obtained in case of Ahmedabad. Increasing trends have been obtained for Bangalore, Varanasi and Srinagar by 0.40, 0.15 and 1.18% per year, respectively. But decreasing trend has been observed at Halley Bay by 3.42% per year. It was also reported that ozone depletion is very high in the Spring time at Halley Bay for a definite year and also from year to year as compared to Indian stations.

6. Effect of green house gases on global warming and ozone depletion

Carbon dioxide (CO_2), methane (CH_4), nitrousoxide (N_2O), chlorofluoro carbon-11 ($CFCl_3$) and chlorofluorocarbon-12 (CF_2Cl_2) gases have strong absorption band at 8–20 μm [157,158]. Ozone also absorbs infra-red radiation [159]. These gases are thus more effective green house molecules in the atmosphere.

Atmospheric concentrations of most of the green house gases are continuously increasing. It is reported that CO_2 is currently increasing at 0.5% per year, CH_4, N_2O, CFC-11 and CFC-12 at 0.9, 0.25, 4 and 4% per year respectively [160]. Increased concentrations of green house gases play a key role in global warming. Houghton [161] reported that global surface air temperature has increased about 0.5°C during 20th century. Harris and Chapman [162] showed that for south-eastern Utah, the magnitude of warming from 19th century base line from 1951 to 1970 is 0.6°C and the most recent warming yields a total of 1°C warming from 1990 to 1994 mean.

Because contemporary climate models show a linear increase in temperature and other variables, the future increase should be a linear extension of these recent trends. Thus, it is concluded that the bottom line is a warming of around 1.5°C to 1.7°C in the Winter half year and 1.2°C to 1.3°C in the Summer over the course of the next century [163].

The Kyoto Protocol will have no effect because CO_2 emissions will continue to increase. As a result, the Earth's average surface temperature will increase by 0.65 to 0.75°C in the Winter half year and by 0.60 to 0.65°C in Summer by the year 2050 [163].

Huang *et al* [164] used present-day temperatures in 616 bore holes from all continents except Antarctica to reconstruct century-long trends in temperatures over the past 500 years at global, hemispheric and continental scales. The average of the cumulative temperature change over the five-century interval is a warming of about 1.0 K, and the twentieth century has been the warmest century of the past five. Almost 80% of the net temperature increase has been observed in the nineteenth and twentieth century. The magnitude of ground surface warming over the past five centuries is greater in the Northern Hemisphere than in the Southern Hemisphere : The five century cumulative change is 1.1 K in the former and 0.8 K in the later. The twentieth

century temperature change is 0.6 K in the Northern Hemisphere and 0.4 K in the Southern Hemisphere. These values compare, respectively, with 0.60 and 0.65 K per century for hemispheric trends in the combined land and sea surface air temperature [165]. The geothermal hemispheric estimates for the twentieth century show even greater consistency with the land —only hemispheric trends of 0.56 and 0.47 K per century [166]. The five-century cumulative temperature changes are respectively 1.2 K for North America, 1.4 K for South America, 0.8 K for Europe, 0.8 K for Africa, 1.2 K for Asia and 0.5 K for Australia [164].

Macilwain [167] reported that according to the conclusion of the NRC (US National Research Council) panel, an increase in global mean surface temperature over the past 20 years "is undoubtedly real and is substantially greater than the average rate of warming during the twentieth century". CO_2 contributes ~45% of all green house forcing [168,169]. CO_2, CH_4 and N_2O account for about 70% of anticipated global warming [168]. N_2O contributes about 15% of radiative forcing of CO_2 [170]. Again it is observed that CH_4 and N_2O concentrations are much samller than for CO_2. But these contribution to radiative forcing per molecule change is about 20 times more important for CH_4 than for CO_2 and 200 times for N_2O [171].

On the other hand, increased concentration of green house gases cause lower stratosphere cooling by radiating heat to space creating 'an ice house effect' [172]. It enhances the formation of polar stratospheric clouds (PSCs) which increases depletion of ozone. It can be supported by the following facts. Ramaswamy *et al* [173] showed that the global mean cooling in the ~50–100 hPa (~16–21 km) lower stratospheric region, due to increase in CO_2 alone since 1979–1990 is ~0.6 K, due to increase in all other green house gases for the period of 1765–1990 is about 0.15 K. Austin *et al* [55] further showed that over Northern Hemisphere Winter stratosphere, doubling CO_2 concentration leads to the formation of an Arctic ozone hole comparable to the observed over Antarctica with nearly 100% local depletion of lower stratospheric ozone. Moreover chloroflurocarbons by absorbing UV-radiation release active atomic chlorine which catalyses ozone depletion shown by Molina and Rowland [91], Molina and Molina [92] and McElroy *et al* [97]

$$CFCl_3 + h\nu \rightarrow CFCl_2 + Cl \ (\lambda < 230 \text{ nm}),$$

$$CF_2Cl_2 + h\nu \rightarrow CF_2Cl + Cl \ (\lambda < 230 \text{ nm}).$$

H_2O vapour is also one of the green house molecules. By photodissociation, it forms OH radicals. OH radicals thus formed, can react with CO or CH_4 to produce HO_2 radicals [90]. These radicals directly catalyse O_3 depletion as shown by Solomon *et al* [99] and upper stratospheric and mesospheric ozone depletion reported by Summers *et al* [45].

7. Special features of Antarctic region and future of ozone hole

In the both southern and northern polar region, stratosphere starts from a relatively lower altitudes of 8 km and maximum ozone concentration occurs between 15 and 20 km altitude. Both the polar regions experience many weeks of continuous darkness, polar night during Winter from May to August in Antarctica. Southern polar region (Antarctic region) experience stratospheric minimum temperatures during Winter, special circulation patterns, intense and strong winds and different meteorological conditions.

The temperature of the stratosphere at 50 mb pressure over Antarctica during winter drops to –80°C which is nearly 20–30°C lower than that over arctic region [174]. The amount of time that the stratosphere is such cold, is several months for Antarctic and few weeks for other regions. For example, it was ~5 months for Southern Hemisphere and ~6 weeks for the Northern Hemisphere during the 1991-1992 Winter seasons [41]. At this temperature, PSCs are formed which disappear in early November following the rise of temperature. The formation of PSC is more frequent in Antarctica than in arctic region. The polar vortices are usually centred over eastern Antarctica. They are more intense due to low temperature and strong winds and stable than its arctic counter part. The Antarctic polar vortices do not break down before Spring and are probably related to stratospheric warming. At ~190 K, type II ice PSCs can form and sediment out of the stratosphere, removing HNO_3 as a source for NO_2 to quench ClO and reduce ozone destruction [175,176]. Type I PSCs can also grow sufficiently large under suitable condition [175] to sediment and remove HNO_3. Thus, stronger ozone depletion can be expected in Antarctica during Spring as a result of increased concentrations of reactive chlorine and bromine species, low concentrations of nitrogen oxides, large occurrence of PSCs and very low temperature. Consequently, ozone hole will extend its size and will be much deeper.

The Antarctic ozone hole is mainly confined to the region of lower stratospheric temperature remaining below –78°C for several months with frequent PSCs inside the polar vortex. The areal extent of the –78°C region is governed by planetary wave activity occurring during the Fall and Winter, before the Spring time. So the maximum size of the Antarctic ozone hole should be fixed by the size of the core of cold temperature in the vortex, which locates the CPR (Chemically perturbed region) and then by dynamical boundary of the polar vortex [177].

The Arctic ozone depletion occurs in regions where PSC appearance is more episodic than continuous. The Arctic chemical perturbation and extra-CPR Antarctic depletion is

greatly influenced by intermittent PSC appearance associated with tropospheric cyclonic uplift or internal gravity waves. As the concentrations of stratospheric reservoir chlorine compounds continuously increase, the intermittent processing will increase concentrations of Cl radicals. The Arctic vortex and extra Antarctic CPR will experience increased ozone loss. If the Antarctic ozone depletion reaches the dynamical vortex boundary, then ozone hole will effectively double in area, since the CPR currently occupies only about half the present area of the Antarctic vortex. The Arctic vortex covers about half the area of Antarctic vortex in the respective spring seasons and the coldest regions are between 20 and 50 mb. Thus, the most severe Arctic ozone hole will never arise unless stratospheric climate or water vapor content changes. Stratospheric climate is mainly controlled by the radiative balance between heating through absorption of UV-radiation by ozone and cooling though the emission of IR-radiation by green house molecules. The polar vortex becomes colder, larger and more persistent through radiative processes, either by reduced solar absorption by O_3, or by more efficient emission of thermal energy by green house molecules. So the increased O_3 loss, increased concentration of green house molecules and the vigorous mixing provided by large amplitude planetary waves that propagate upward from troposphere may cause significant amplification of the Arctic ozone hole as well as deeper Antarctic ozone hole. It is shown in Figure 5 that ozone hole in 1998 at Antarctica is much deeper (grey region) than the ozone hole in 1996.

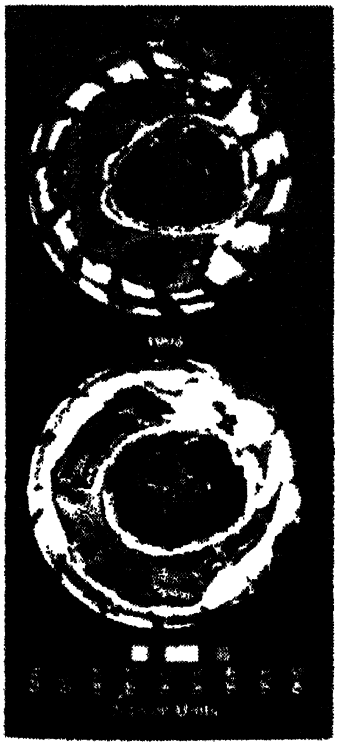

gure 5. Antarctic ozone hole in 1996 and 1998.

8. Effect on solar UV-radiation

The solar radiation at the top of the Earth's atmosphere has a significant amount of energetic shorter wavelength radiation. Wave-length in the range 100–400 nm is called the ultraviolet (UV) spectral region. There are three types of UV-region : UV-A, UV-B and UV-C. Wavelength in the range 100–280 nm is known as UV-C region. It is completely absorbed by atmospheric oxygen (O_2) and ozone (O_3). Wavelength in the range 280 nm–315 nm called UV-B region are partially absorbed by O_3 but not completely, while UV-A wavelengths (315–400 nm) are absorbed only weakly by O_3 and are therefore more easily transmitted to the Earth's surface. At the equator, about 30% of the middle UV-B region of solar radiation are transmitted to the Earth's surface under clear sky [67]. Ozone depletion increases the solar UV-B radiation reaching the ground [178]. High levels of UV-B radiation have been observed directly in association with the Antarctic ozone hole [179–182].

Total stratospheric content of ozone depleting substances (ODS) is expected to reach a maximum around the year 2000. All other things being equal, the current ozone losses and related UV-B increases should be close to their maximum. The temporal change of ozone and surface UV-radiation (at 45°N and 45°S) computed in correspondence to the halocarbon loading of the atmosphere are shown in Figure 6 assuming that changes in UV-radiation are due solely to ozone changes which in turn are assumed to

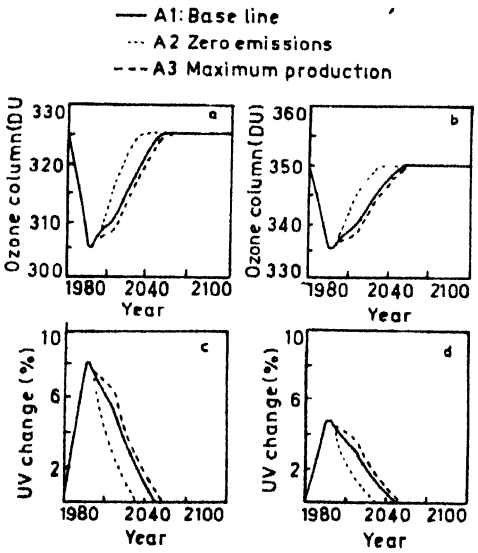

Figure 6. Scenario for future changes in ozone and erythemal UV-radiation at the Earth's Surface, at 45°N (b, d) and 45°S (a, c).

response only to atmospheric halocarbon loading [183]. The quantitative relation between ozone and halocarbon changes is based on the measured changes in both quantities through the 1980s [184]. The future scenarios shown in the figure are based on current control measures (Montreal 1997 Amendments). In scenario A_1, the production of some ODS

is already below the allowed maximum level, while under scenario A_3, the production is at the maximum allowed level. Scenario A_2 shows the ozone/UV-recovery if there is no emission after the year 2000.

9. Effect on sunburn and skin cancer

Direct exposure to UV-B radiation has acute undesirable effects including sunburn and skin pigmentation consisting immediate pigment darkening (IPD), neomelanogenesis and the chronic effects. It is more conspicuously seen in the cancasions, resulting thickening of the epidermis damage to dermis (solar elastosix) [185]. Patients lacking pigment (albinos) or having a defective DNA dark repair mechanism (Xeroderma pigmentosum) tend to develop cutaneous malignancies more frequently and more readily. Nutritional deficiencies such as that of vitamin B_3 (nicotinic acid) can result in photosensitive dermosis. It was also reported that melanin is the most important natural protection against damage from sunlight. The production emission of ozone depletion substances (ODS) through ozone depletion increases in carcinogenic UV-radiation, which increases the skin cancer incidence. Slaper *et al* [186] evaluated three types of skin cancer. Squamous cell carcinoma (SCC) and basal cell carcinoma (BCC) are the most frequent but least aggressive. The cutaneous malignant melanoma (CMM) is the least frequent but most aggressive [187]. Scotto and Fears [188] reported that the present skin cancer incidence in the USA is about 2000 per million per year and in North-West Europe an incidence of about 11,000 per million per year for the Netherlands as representative [189]. Slaper *et al* [186] showed the relative increase in effective yearly UV-dose received at ground level at 40°N (USA) and corresponding the excess skin cancer incidences in USA for the period 1975-2100 in Figures 7, 8(a) and 8(b). They predicted that

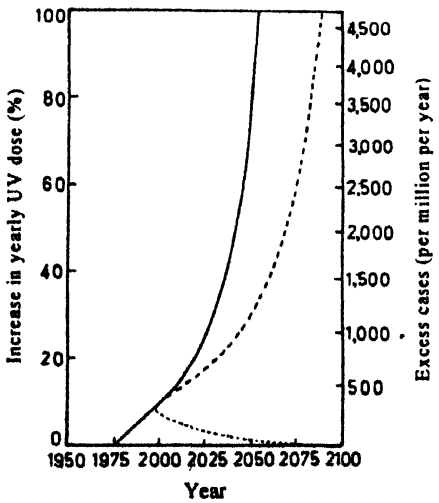

Figure 7. Relative increase in yearly effective UV-dose received at ground level at 40°N (USA). The solid line represents no restrictions (NR) scenario, the broken line the Montreal Protocol (MP) scenario and the dotted line the Copenhagen Amendments (CA) scenario.

in the CA (Copenhegan Amendments, 1992) scenario, the calculated number of excess cases caused by ozone depletion will exceed 33,000 per year in the USA around the year 2050 and 14000 per year in North-West Europe.

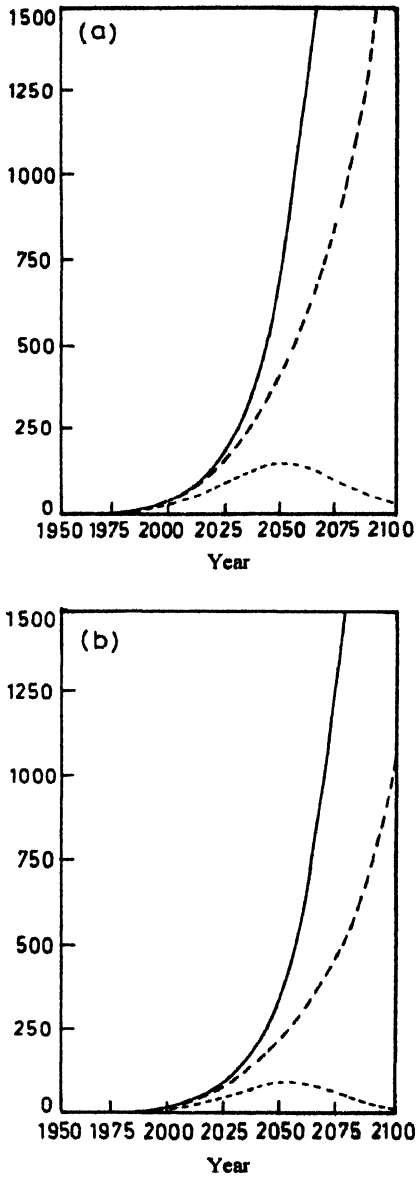

Figure 8. Excess incidences calculated for the USA (a) and northest Europe (b) populations, incorporating the delay between exposure and the occurrence of tumours. The solid line represents the NR scenario, the broken line the MP scenario and the dotted line the CA scenario.

Squamous cell carcinoma (SCC) associated with ambient solar exposure has been reported in catle, horses, cats, sheep, goats and dogs [190–192]. These tumors occur principally in poorly pigmented skin unprotected by hair and thus are frequently found on eyelids, nose, ears, tails, the mucocutaneous junctions of the eyes and anogenital regions [192]. Other effects in domestic animals include exacerbations of infectious bovine keratoconjuntivitis in cattle [193] and skin lesions and cataract in farm raised-fish [194]. Increases

in surface erythemal (Sun burning) UV-radiation relative to the values in the 1970's are estimated to be : about 7% at Northern Hemisphere mid latitudes in winter/spring; about 4% at Northern Hemisphere mid latitudes in summer/fall; about 6% at southern Hemisphere mid latitudes on a year-round basis; about 130% in the Antarctica in spring and about 22% in the Arctic in spring due to ozone losses by 50% in the Antarctic spring, 15% in the Arctic spring, 6% at Northern hemisphere mid latitudes in winter/spring, about 3% at Northern Hemisphere mid latitudes in summer/fall and about 5% at southern hemisphere mid latitudes year-round. The corresponding increases in erythemal UV radiation are estimated to be 130, 22, 7, 4 and 6% [183].

10. Effect on eyes

The eye is a principal route of exposure to UV radiation. When sunlight containing UVR falls on the normal eye, the cornea is affected first, followed by the lens, the vitreous humor and the retina. Due to absorption by various molecules in the cornea and the lens, most UV-radiations never reach the ratina in the normal adult eye. The cornea absorbs most of the UV-radiation below 300 nm. The lens absorbs almost all of the rest ambient UV-radiations below about 370 nm [195].

The ocular effect due to environmental exposures to UVR is photo keratitis. It is characterized by reddening of the eye ball, gritty feeling of severe pain, photophobia and blepherospasm or twitching. Photokeratitis is also seen in beach-goers and others involved in outdoor recreation [196]. Additional ocular effects are climate droplet keratopathy (CDK), pinguecule, pterygium and squamous cell carcinoma (SCC) of the cornea and conjunctiva. Climate droplet keratopathy is a degeneration of the fibrous layer of the cornea with the accumulation of droplet-shaped deposits. Pterygium results from an outgrowth of the conjunctiva over the cornea, which results in the loss of transparency, pinguecule is a raised opaque mass just adjacent to the cornea [197] and squamous cell cercinoma is a malignant neoplasm.

Of all the ocular diseases associated with solar exposure which affects the lens, cataract is characterized by a gradual loss in the transparency of the lens due to accumulation of oxidised lens proteins [196]; frequently the end result is blindness, unless the affected lens is surgically removed. There are several kinds of cataract. Cortical cataract develops in the outer layers of lens protein, commonly called the cortex of the lens. Nuclear cataracts occur in the inner layer of lens protein *i.e.* the nucleus of the lens. Posterior sub-capsular cataracts (PSCs) occur at the back interface of the lens and its epithalial capsule. Recent Italian-American case control study of individuals aged 45–79 years reveals that pure cortical cataract accounts for slightly less than 50% of cases, Pure nuclear cataract accounts for about 10%, pure PSC for less than 3% and mixed for about 40% with the majority of the mixed having a cortical component [198,199].

11. Effect of tropospheric ozone and lung function

In urban and industrialized regions, tropospheric ozone is formed by the photochemical reactions of some pollutants *e.g.* oxides of nitrogen, hydrocarbon while in remote regions it stems from both downward transport from the stratosphere and from *in situ* photochemical production from source regions [200].

Tropospheric ozone is an effective absorber of UV-B radiation [201]. In industrial regions of the Northern Hemisphere, the increases in tropospheric ozone since pre-industrial times may have reduced DNA-damaging UV-radiation by 3–15% [201–205].

The lower UV-radiation levels observed in Germany may be explained partly by higher tropospheric ozone levels [206]. Increase in tropospheric ozone causes climate change through global warming, environmental pollution and also affect human health. According to Fishman [207], long term tropospheric ozone analysis shows an increasing trend at a rate of 1–2% per year recently in the Northern Hemisphere. This tropospheric O_3 increasing concentration causes greater global warming comparable to the increase of CO_2. Besides O_3 is toxic and causes serious environmental damage as well as impairment of human health. Berry *et al* [208] reported that accumulated exposure to ozone concentration greater than 120 ppb had an increase in respiratory symptom. Peak expiratory flow rate in children was the only lung function measure associated with increasing ozone concentrations with an average loss of 4.74 ml/s/ppb for the eight hours ozone exposure. The early intense exposure to O_3 produced a persistent decrease in lung function and base line shifts for 3 days after the episode that obscured daily dose-response relationship. Spector *et al* [209] reported that O_3 exposures in ambient air produced greater lung function deficits in active young people in natural setting than does pure O_3 in controlled chamber exposure studies because of longer exposure and potentition by other factors. Chen *et al* [210] investigated the ozone pollution in the environment and its health effect on the population. They reported that the O_3 concentration in the air in Nanjing city, China, was ≤ 0.069 mg/m^3. The concentrations in O_3 lamp rooms, UV-lamp room and photocopy machine rooms were 1.289, 0.245 and 0.01–0.03 mg/m^3 respectively. The lung function indicators of the O_3 exposed population differ significantly from those of the controls. Whitefield *et al* [211] assessed the qualitative and quantitative judgements regarding the risk of chronic lung injury to children aged 8–16 and adult out-door workers

due to long term O_3 exposure in areas with patterns of exposure similar to those in Southern California and the northest. Ozkaynak *et al* [212] showed that O_3 exposure was associated with increased pneumonia and influenza in adults after a 24-hour lag period. Cody *et al* [213] analysed the data on hospital emergency department visits for May through August for 1988 and 1989 in New Jersey. It was shown that asthma visits were correlated with temperature whereas the correlation between asthma visits and O_3 concentration was nonsignificant. However when temperature was controlled for in a multiple regression analysis a highly significant relation between asthma visits and O_3 concentration was identified. Also in Canada, the contribution of O_3 to asthma admission was stronger in areas with higher concentration. Manning *et al* [214] studied the O_3 injury to native plants in class 1 wilderness areas in Vermont and New Hampshire. Symptoms of O_3 injury were confirmed for black cherry, milkweed, whiteash, white pine and two species of black berry.

12. Effect on bacterioplankton, picoplankton, cyanobacteria, phytoplankton and zooplankton and secondary consumers

12.1. Dissolved organic substance :

Solar UV-radiation can degrade most of the dissolved organic Carbon (DOC) photolytically [215]. Humic substances after photolytic degradation are readily taken up by bactrioplankton [216]. Humic substances strongly absorb UV-radiation. Thus, UV-B penetration into water column is increased by the increased degradation of DOC and subsequent consumption by bacteria. Close to the surface, DOC is rapidly photolysed and bacterioplankton activity is inhibited by solar UV-radiation. DOC photolysis generates photosensitizers which on absorption of UV-radiation produce reactive oxygen species (ROS) or free radicals.

Pienitz and Vincent [217] found large shifts in UV-B, UV-A and photosynthetically available radiation, associated with changes in the input of coloured dissolved organic material into subarctic lakes during the holocene. The inferred changes in biological exposure to UV-radiation were at least two orders of magnitude greater than those associated with moderate (30%) ozone depletion. Fresh water ecosystems at present located across vegetation gradients will experience significant shifts in under water spectral irradiance through the effects of climate change on catchment vegetation and the export of coloured dissolved organic material.

12.2. Bacterioplankton and picoplankton :

The effect of solar UV-radiation in case of bacterioplankton depends on the spectral attenuation coefficient in the water column, the time pattern of exposure and protection for the organisms since they are passively moved in the mixing layer. Bacterioplankton lack UV-screening pigments e.g. mycosporines or scytonemins possibly due to their tiny size [218,219]. Consequently bacterioplankton are more prone to UV-stress than larger eukaryotic organisms. UV-exposure produces about double the amount of cyclo-butane dimmer as shown in a case study in the Gulf of Mexico [220,221] Solar UV-B radiation affects other macromoleculer parts of the bacterial cells as well as ectoenzymes responsible for the cleavage of external organic compounds [222]. The bacterioplankton serve as food for heterotrophic picoplankton (< 1 μm). The bacterio-plankton abundance is limited by UV-damage, viruses and heterotrophic flagellates [223,224], UV/blue radiation (360–430 nm) is most effective in the induction of the activity. The viruses and nanoflagellates show a high sensitivity to solar UV-radiation [225].

12.3. Cyanobacteria :

Cyonobacteria, a group of prokaryotes possessing a higher plant-type oxygenic photosynthesis use the nitrogenase enzyme to reduce atmospheric nitrogen into ammonium ions (NH_4^+), which they make available for aquatic eukaryotic phytoplankton as well as higher plants [226–229]. UV-B affects the processes such as growth survival, pigmentation and motility as well as the enzymes of nitrogen metabolism and CO_2 fixation [230,231]. Growth and survival decrease within a few hours of UV-B radiation depending on the species.

The phycobiliproteins are readily bleached and cleaved [227,232,233]. Bleaching of these additional pigments is far more efficient than that of chlorophylla or carotinoids [232] At lower doses, the energy transfer to the reaction centre of photosystem II is impaired [227]. Simultaneously with destruction, an increased synthesis of phycobiliproteins has been observed under mild UV-stress. These pigments strongly absorb UV-B. They form a peripheral layer around the central part containing the DNA. It indicates that phycobilins are effective screening pigments [233] as well. They are capable of intercepting more than 99% of UV-B radiation before it penetrates to the genetic material. Sinha *et al* [227] reported that in addition to the bleaching of photosynthetic pigments, RuBisCO (ribulose-1, 5-bis-phosphate carboxylase/ oxygenase) activity was severely affected by UV-B treatment. Ammonium uptake was reduced by 10% in cultures exposed to solar radiation. The nitrogen fixing enzyme nitrogenase is inhibited by UV-B even after a few minutes of *in vivo* exposure. A complete loss of activity was found within 35–55 min. depending on the species [234] possibly due to the inhibition of ATP synthesis by UV-B. In contrast to the effect on nitrogenase, a stimulation of nitrate reductage by

UV-B was found in all nitrogen-fixing cyanobacterial strains [232], while the ammonia assimilating enzyme glutamine synthetase (GS) was inhibited.

Screening pigments include scytonemin and MAAs, as well as a number of spectroscopically characterized but chemically unidentified water soluble pigments [234,235]. Cyanobacteria such as scytonema and Nostoc form filaments that lie embedded in a mucilaginous sheath. The screening pigment from scytonema hofmannii shows an absorption maximum at 314 nm and is released into the medium during the late stationary phase of growth. These organisms are more tolerant of UV-B irradiation than those which do not contain such covering [232]. For example, other scytonema species, which do not produce this pigment are unable to survive in two hours of UV-irradiation (2–5 Wm^{-1}). Kirsten and Garcia-Pichel [236] showed that screening pigments such as scytonemins, carotinoids and MAA are incorporated into the cytoplasm or the outer slime sheath, efficiently protecting the organisms from solar short-wavelength radiation.

12.4 Phytoplankton :

Phytoplanktons, the most important biomass producers in aquatic ecosystem populating at the top layers of the oceans and fresh water, called euphotic zone, receive sufficient solar radiation for photosynthetic processes. Solar UV-radiation affects growth and reproduction, photosynthetic energy-harvesting enzymes [237–243] and other cellular proteins, as well as photosynthetic pigment contents [244–247] The uptake of ammonium and nitrates is affected by solar radiation in phytoplankton [248–251] as well as in macroalgae [252]. Solar UV-B has been found to induce DNA damage and DNA Synthesis delay in many organisms [253–256].

12.5. Zooplankton :

Phytoplankton concentrations depend on nutrient availability, light, temperature, UV-stress and strongly on the grazing losses by zooplankton activity [257]. The zooplankton concentrations depend on phytoplankton availability, grazing pressure as well as solar UV and temperature. The macrozooplankton biomass in the California currently had decreased by 80% since 1951, due to climatic warming by more than 1.5°C in some places [258]. As in phytoplanktons UV-B induced DNA damage and photoenzymatic DNA repair have also been demonstrated in zooplankton [259]. In planktonic embryos of copepods photoreactivation of UV-induced damage was found to be an efficient repair mechanism [260]. However, UV-B severely affects survival, fertility and sex ratio in several intertidal copepods while others remain largely unaffected [261].

12.6. Secondary consumers :

Sea urchins and corals are also UV-B sensitive marine organisms [262,263]. The planula larvae of the coral Agaricia agaricites are known to show a clear variation in the UV-B sensitivity along a depth gradient [264] and the green sea Urchin Strongytocentrotus droebachiensis uses a MAAs that it derives from its diet for UV absorption. This latter adaptation was determined by feeding an MAA-rich red alga, Mastocarpus stellatus and MAA-deficient brown alga, laminaria saceharina to sea urchins [265].

The eggs and larvae of many fish are sensitive to UV-B exposure [266–268]. Ambient UV-levels in the surface waters of temperate lakes are adequate to induce 100% mortality of yellow perch eggs in low-DOC lakes but not in lakes of higher DOC levels [269].

Worrest and Kimeldorf [270] reported several adverse effects of increased exposure to UV-B radiation on the systemic development of boreal toad (Bufo boreas boreas) tadpoles in the laboratory. It was found that DNA damage in pelagic fish eggs and larvae increases as the sun rises, reaches a peak level of damage near solar noon and is followed by a period of rapid repair in the afternoon when UV-B decreasing, but the visible light utilized for repair is still abundant.

13. Effect on atmospheric concentrations of HO*x*, (CH_4), (CO) and (H_2O_2)

13.1. Changes in HOx :

HOx radicals (OH and HO_2) play an important role in tropospheric chemistry. Important sources of these radicals are the photolysis of ozone, hydrogen peroxide (H_2O_2), formaldehyde (HCHO) and several other inorganic and organic species. Increased UV-B actinic fluxes yield higher tropospheric concentration of the HOx radicals.

Calculation done by Fuglestvedt *et al* [271] clearly shows that the increases in UV-B radiation over 1979–1993 have led to an increase of OH concentration on the global scale of about 8%, with the largest fractional increases (~40%) found for high southern latitudes in October. Ma [272] reported that potential changes in the concentrations of OH, HO_2 and CH_3O_2 in the troposphere for a 10% reduction of stratospheric ozone. The OH concentration is predicted to increase by 8–9% in the lower troposphere over global scale. The HO_2 and CH_3O_2 concentrations are predicted to increase by about 4–6% respectively, due to the increased oxidation rate of CO and hydrocarbons by OH. Prinn *et al* [273] found no statistically significant trend in OH concentration over 1978–1990. A re-analysis of the methyl chloroform data [274] suggests a slight positive OH trend of about 0.4–0.5% per year over 1978–1993.

13.2. Changes in atmospheric concentration of CH_4 and CO :

The atmospheric concentrations of CH_4 and CO are determined by the balance between emission sources and atmospheric removal, mostly by OH radicals. An important additional source for CO is the atmospheric oxidation of CH_4 and other hydrocarbons [275].

Analysis of polar ice cores [276] indicates that pre industrial atmospheric methane concentration was about 650 ± 40 ppb. Atmospheric CH_4 concentration started to increase about 100 years ago. The rate of increase was approximately 16 ppb per year in the late 1970s, while in the later part of the 1980s, the increase was about 9 ppb per year. Increased UV-B radiation is expected to cause higher levels of OH, correspondingly faster loss of methane is expected.

Carbon monoxide concentration measurements indicate an increase in the CO abundance of 1% per year over the past forty years in the Northern Hemisphere [277] and no significant trend in the Southern Hemisphere [278]. A large decrease in the CO concentrations was observed between 71°N and 41°S during June 1990–June 1993, with a decrease of 15–18 ppbv at most stations located north of 25°N, and of 8–12 ppbv between 41°S and 20°N [279]. Increases in OH concentration is expected in association with stratospheric ozone depletion, global decreases in CO concentration are thus expected. Granier *et al* [280] concluded that changes in total ozone abundance may be responsible for global decreases in CO of about 3.5 and 1.7 ppbv in the Northern and Southern Hemispheres, respectively accounting for about 20% of the observed CO decrease.

The volcanic eruption of Mount Pinatubo (Philippines) on 15 June, 1991 emitted approximately 20 Mt. of SO_2 and 3–5 km^3 of ash into the upper troposphere and lower stratosphere. A radiative transfer model calculation shows that the tropospheric UV-B actinic flux in the tropics was reduced by about 12% immediately after the eruption due to direct absorption by SO_2 and was perturbed for upto one year after the eruption due to scattering by sulphate aerosols [281]. This study suggested that the decreased UV-B flux caused a decrease of OH concentration and therefore led to the observed anomalously large growth rates for CH_4 and CO during late 1991 and early 1992.

13.3. Changes in H_2O_2 concentration :

Hydrogen peroxide (H_2O_2), one of the principal oxidants in the troposphere plays a key role in the aqueous phase oxidation of SO_2 to SO_4^{-2}. Model calculations suggest that tropospheric H_2O_2 concentrations should increase in response to enhanced tropospheric UV-B actinic fluxes, in parallel to the expected increases in HOx radicals, (especially HO_2). The H_2O_2 concentration is greatest in low NOx regions where the formation of peroxides is the pre-dominant fate of HOx radicals. 50% increase in H_2O_2 concentration was observed at Eurocore (Central Greenland, 72°N) in the firm/ice during the last 200 years, with most of the increase having occurred between 1960 and 1988 [282]. Recent studies at Summit, Greenland (72°N) in 1995 clearly indicates that H_2O_2 increases in ice cores and a further increase of the H_2O_2 concentration is being observed since 1988, leading to an overall increase of 60 ± 12% during the last 150 years [283]. Photochemical model calculations for Summit [284] suggest that ozone depletion over 1980-1990 (from 395 to 360DU) produces an atmospheric H_2O_2 increase of about 7% for Summer which could account for about one third of the increase observed over that time period.

14. Effect on synthetic and naturally occurring polymers

Synthetic polymers (*e.g.* plastics) as well as naturally occurring polymer (*e.g.* wood) are extensively used in building construction and other applications. Various applications of polymers are shown in Table 2. The UV-B content in sunlight is well known to affect adversly the mechanical properties of these materials, limiting their useful life [285]

Table 2. Plastic materials routinely exposed to solar UV-radiation.

1.	Building applications	Plastic window and door frames, siding, mobile-home skirting, gutters and downspouts, conduits, cable covering, flooring, outdoor furniture Exterior fascia and soffit (rigid PVC). Membrane roofing, geomembranes, weather stripping (Plasticized PVC, EPDM rubber, other rubbers) Glazing, covers for lighting fixtures (Polycarbonate and acrylics). Varnishes and coatings used to protect surfaces Highway marking paints, Resins used in the repair of monuments.
2.	Agricultural applications	Irrigation houses, pipes netting (PE and PVC) Tanks for storage of water (unsaturated polyester and PE). Mulch films and green house films (PE and PVC).
3.	Transportation :	Automobile tires (rubber). Plastic used in automobile, aircraft and marine vessel construction.
4.	Other	Fishing nets, sails, outdoor temporary housing, outdoor furniture, fibers and textiles.
5.	Biopolymers	Wool, human hair, wood chitinavous materials.

PE = Poly ethylene; PP = Polypropylene; PVC = Polyvinylchloride; EPDM = Ethylene-propylene-dienemonomer.

Now-a-days its outdoor lifetimes depend on the use of photostabilizers in the case of plastics and on protective surface coatings in the case of wood. So any increase in the solar UV-content due to more ozone depletion would tend to decrease the outdoor service life of these materials. Schematic diagram of the various stages of light induced damage in polymers and its mitigation is shown in Figure 9.

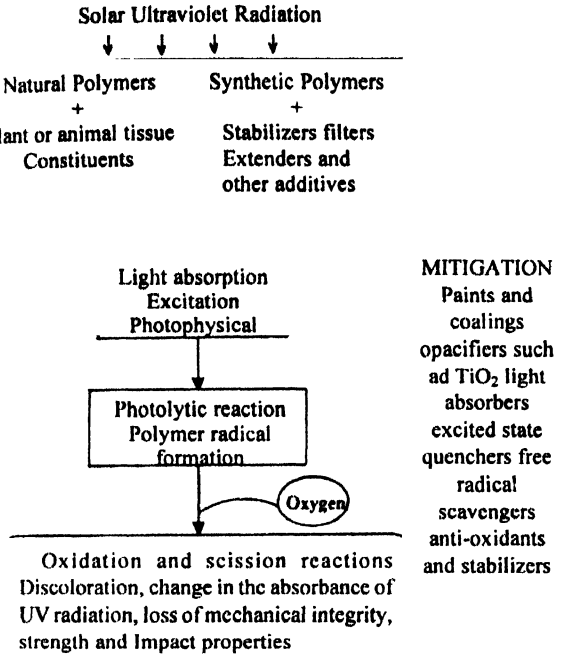

Figure 9. Schematic diagram of the various stages of UV-induced damage in polymers and its mitigation.

15. The Antarctic and Arctic aquatic ecosystem

At high latitude variability in solar elevation, cloud cover, deep vertical mixing and the cover of ice and snow confound field results of UV-B effects on phytoplankton and the consequent interpretation of these results. Recent estimates of the effect of 50% ozone reduction on integral water column productivity are relatively consistent, less than 5% [286] and 0.7–8.5% [287] with earlier estimates (6%) [288]. It is reported by Neale *et al* [289] that an abrupt 50% reduction in stratospheric ozone could, as a worst case, lower daily integrated water column photosynthesis by as much as 8.5%. They also noted that inhibition associated with realistic environmental variability can have a stronger influence on integrated water column photosynthesis than UV-B effects; vertical mixing by about ±37%, measured variable sensitivity of phytoplankton to UV by about ±46% and cloudiness by about ±15%.

There are some differences between the Arctic and Antarctic aquatic ecosystem. The Arctic Ocean is a nearly closed water mass with limited water exchange with the Atlantic and Pacific oceans. It represents 25% of the global continental shelf and receives about 10% of the world river discharge. Another difference between the Arctic and the Antarctic is the greater importance of macroalgae in the Arctic. The Arctic aquatic ecosystem is one of the most productive ecosystems on earth and is a source of fish and crust oceans for human consumption. Both endemic and migratory species breed and reproduce in this ocean in spring and early summer at a time of maximum UV-B radiations.

Productivity in the Arctic Ocean has been reported to be higher and more heterogeneous than in the Antarctic Ocean [290]. In the Bearing Sea, the phytoplankton may experience relatively high level of solar UV-B because of the little depth water and the prominent stratification of the water layer. In addition, important fishes such as herring, pollock, cod and salmon *etc*. produce eggs in shallow waters in presence of this increased solar UV-B radiation. Many of the eggs and early larval stages are found at or near the surface. The high concentrations of humic substances which absorb UV-B strongly may change the under water light penetration significantly. Again UV-B is known to attack humic substances photochemically, alters the absorption nature of the water column and leads to faster uptake by bacteria and heterotrophic nanoflagellates [291]. It is reported that phytoplankton cells larger than 2 μm are twice as sensitive to solar UV-B as smaller cells [292]. The Arctic Ocean is often especially inorganic nutrient limited such as nitrogen and phosphorous. The nitrogen cycle controls the primary productivity of the marine ecosystems. Nitrogen and phosphorous uptake are UV-B sensitive [293], which may increase the UV-B sensitivity of Arctic phoytoplankton communities. Low doses of UV-B increases the phosphate uptake used probably for DNA repair.

16. Environmental effects of ODS substitutes or alternatives

A large number of chemicals are now being used or proposed (Table 3) as substitutes or alternatives for ODS phase out

Table 3. CFC Substitutes and their chemical name.

CFC	Substitutes	Chemical name
1.	FC-3-1-10	Perflurobutane
2.	FC-5-1-14	Perfluorohexane
3.	FM-100	Bromo difluoro methane
4.	HCFC-21	Dichlorofluoro methane
5.	HCFC-124	1-Chloro-1,2,2,2-tetrafluoroethane
6.	HCFC-22	Chlorodifluoro methane
7.	HCFC-141b	1,1-Dichloro-1-fluoroethane
8.	HCFC-142b	1-Chloro-1,1-difluoroethane
9.	HCFC-143a	1,1,1-Trifluoro methane

Table 3. *(Cont'd.)*

CFC	Substitutes	Chemical name
10	HCFC-152a	1,1-Difluoroethane
11.	HCFC-225ca	1,1-Dichloro-1,1,2,2,3-pentafluoropropane
12	HCFC-225cb	1,3-Dichloro-1,1,2,2,3-pentaflouropropane
13.	HFA-132b	1,2-Dichloro-1,1-difluoroethane
14.	HFA-133a	1-Chloro-2,2,2-trifluoroethane
15	HFA-142b	Chloro difluoroethane
16	HFC-23	Trifluoromethane
17	HFC-32	Difluoromethane
18.	HFC-125	Pentafluoroethane
19	HFC-134a	1,1,1,2-Tetrafluoroethane
20.	HFC-227ea	1,1,1,2,3,3,3-Heptafluoropropane

under the Montreal Protocol and its Ammendments. Increased usage of such substitutes may also cause some environmental problem.

Production of Trifluoroacetic acid (TFA) : Among Hydrochlorofluoro-carbons (HCFCs) and hydrofluorocarbons (HFCs), HCFC-123 (CF_2CHCl_2), HCFC-124 (CF_3CHFCl) and HCF-134a (CF_3CH_2F) are expected to degrade to form TFA. TFA can also be produced by the oxidation of other organofluorine compounds released in the atmosphere by human activities *e.g.* halothane and isofluorane anesthatics. TFA is widely used in the chemical industry in processes where it is either consumed or becomes part of a chemical waste stream. Figure 10 shows a generalized scheme for production of TFA through the atmospheric oxidation of halogenated organic compound CF_3CXYH (X = Cl or F and Y = Cl, H, Br or CH_3) [275].

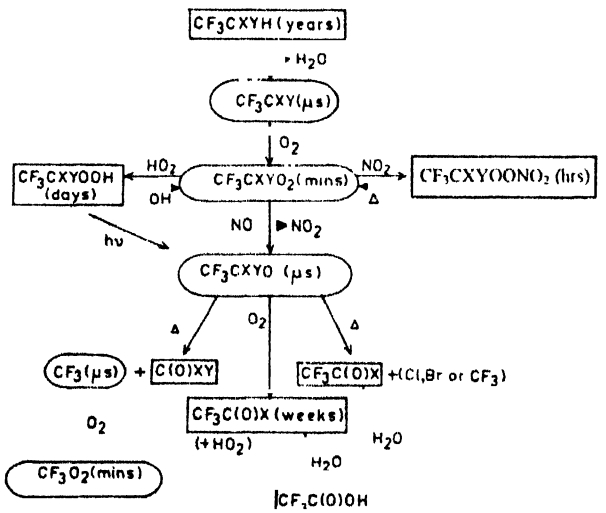

Figure 10. Scheme for the atmospheric oxidation of halogenated organic compound CF_3 CXYH Typical lifetime estimates are given in parentheses.

TFA is a strong organic acid with pKa of 0.23 and easily miscible with water. Trifluoroacetate ion is stable in the aqueous phase and does not undergo chemical changes e.g. hydrolysis, photolysis or formation of insoluble salts. TFA high concentrations have been observed in contemporary water and air samples. Samples of rain and surface water (oceans, rivers, lakes and springs) of USA, Australia, South Africa, Israel, Ireland, France, Switzerland and Finland show that TFA is a ubiquitous contaminant of the hydrosphere [294-297] with values upto 40900 mgl^{-1} [295]. The average TFA concentration in rain water observed in Bayreuth during 1995 was 100 mgl^{-1} [294].

It has been observed that applications of NaTFA at 1000 mgl^{-1} to seeds of sunflower, cabbage, lettuce, tomato, mungbean, soyabean, wheat, coronets and rice do not effect germination [298,299]. The growths of sunflower, soya, wheat, maize, oil seed rape, rice and plantain are not affected by the application of a solution of 100 mgl^{-1} of NaTFA [300]. No effect on growth was observed on plantain at 32 mgl^{-1} of NaTFA, on Triticum and soya at 1 mgl^{-1} and on wheat at 10 mgl^{-1} [301,302].

HTFA is expected to be a severe irritant to the skin [303,304] and to the eye. It is observed that concentrations as low as 2% were moderate skin irritant. It is reported that TFA can cause increased liver weight and induction of peroxisomes [305,306].

All three HFA-132b, -133a and 142b have a low acute inhalation toxicity. HFA-133a has moderately high toxicity to most systems upon repeated exposures with a No Observed Adverse Effect Level (NOAEL) of 24000 mg M^{-3}. All three HFCs, -32, -125 and -134a have low toxicity upon acute and repeated inhalation exposure in standard toxicological testing protocols.

All three HCFCs -21, -124 and -141b, have low acute inhalation toxicity and HCFC-124 and -141 have generally low toxicity overall. The recommended occupational standard for these two HCFCs is 1000 ppm. HCFC-21 demonstrates greater toxicity than the other two HCFCs, with liver toxicity and cardiac sensitization at relatively low concentrations of 15 and 1000 ppm, respectively. The recommended occupational standard for HCFC-21 is 10 ppm [307].

17. Altitudinal distribution of ozone, its age and effects of solar parameters on Antarctic ozone depletion

Midya *et al* [308] in 1995 established an empirical equation theoretically between the variation of ozone concentration and time at a definite altitude considering several ozone formation and depletion processes. It is shown that ozone concentration will decrease very minutely with time for normal atmosphere when [O], [O_2] and UV-radiation remain unaltered. Different rate constants for different reactions involved in ozone formation and depletion are also calculated.

From this empirical equation the approximate age of ozone in the atmosphere of the Earth is calculated by Jana and Midya [309] in 1996. It is shown that the average age of atmospheric ozone is 1.36×10^7 years. It is also reported that altitudinal variation of nitric oxide follows nearly the same trend of altitudinal variation of ozone concentration up to the altitude of nearly 77 Km. Afterwards it follows an opposite trend.

Midya *et al* [310] in 1999 reported that yearly variation of Antarctic ozone concentration in DU (Dobson Unit) and solar flare numbers are mainly controlled by their October concentrations. The nature of variation of O_3 concentration with solar flare number is oscillatory and ozone concentration has slightly increasing tendency with increase of solar flare numbers. Midya *et al* [311] in 2000 established empirical relations between different green house gases and obtained long period data of different green house gases from known concentration of CO_2. They showed from mathematical analysis that percentage contribution of N_2O in O_3 depletion is maximum. In another communication, Midya *et al* [310] in 2000 showed that dramatic decrease of O_3 concentration at Antarctica is independent of solar flare numbers [310], relative sunspot numbers [312], solar UV-flux [313] and solar flare index [314]. It was also shown by Midya and Midya [315] that Antarctic O_3 concentration varies in oscillatory manner with solar flare numbers. Maitra *et al* [316] showed that the variation of ozone concentration is independent of 10.7 cm solar flux. Midya *et al* [317] reported that the intensity of lithium (6708 Å) also decreases with the depletion of ozone concentration over Antarctic survey stations.

18. Montreal protocol in India

It is now well accepted that ozone is depleted everywhere year to year particularly at Antarctica. It is also clear from Figure 11 for the station Halley Bay (76°S, 27°W).

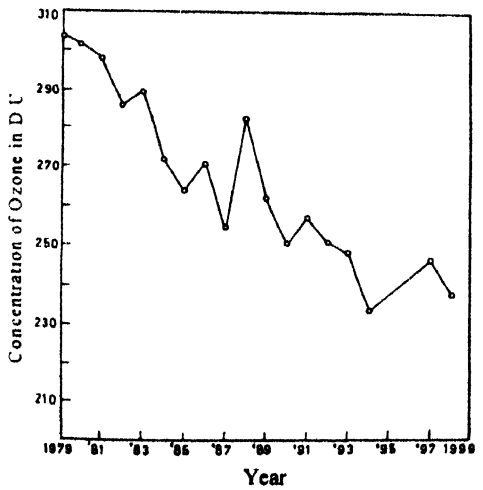

Figure 11. Ozone variation during 1979–1998 at Halley Bay (76°S, 27°W), a British Antarctic Survey Station.

Ozone concentrations are obtained from internet (website http://jwocky.gsfc.nasa.gov). Farman *et al* [1] also reported the dramatic decrease of atmospheric ozone during Antarctic spring time over Halley Bay (76°S, 27°W), a British Antarctic Survey Station (Figure 1). Now ozone depletion is a unique environmental problem. This problem threatens not only human species, but also plants and other animals and requires very urgent international action.

India became a party to the Vienna convention on 19th June, 1991 and the Montreal Protocol on substances that deplete ozone layer (ODS) on 17th September, 1992. The Ministry of Environment & Forests (MOEF) became the coordinating agency in India for all matters relating to the Montreal Protocol. The MOEF appointed its ozone cell as the National Lead Agency for preparation of the country programme. The ozone cell has proposed its country programme with assistance from the United Nations Development Programme (UNDP), the Tata Energy Research Institute (TERI), New Delhi, ministries, representatives of Industry and Scientific Institutions.

Country programme covers the following important and most effective aspects :

(i) To survey and investigate the number and present status, geographical location *etc.* of the sectors and subsectors of industrial using ODS.

(ii) To assess the path of conversion from ODS to non-ODS.

(iii) To suggest phase out options, evaluation, assessment and selection of appropriate technologies relevant to small scale, small and unorganised sectors, demonstration, promotion of these technologies and practice to ODS phase out.

(iv) To estimate the reduction in ODS consumption due to phase out, the production of ODS and the requirements of ODS substitute for a definite period.

(v) To train personnel of all categories involved in different activities in such sectors and subsectors.

(vi) Facilitating project formulation and reviewing and also monitoring the implementation of phase out in the sectors.

India commonly produces and uses seven of the twenty substances under the amended Montreal Protocol.

Annex A.	Group I	CFC-11 (CCl_3F) CFC-12 (CCl_2F_2) CFC-113 ($C_2Cl_3F_3$)
Annex A.	Group II	Halone-1211 Halone-1301
Annex B.	Group II	Carbon tetrachloride (CTC) (CCl_4)
Annex B.	Group III	Methyl chloroform (MCF) (CH_3CCl_3)

Different sectors and subsectors in India are identified which use ODS. Alternatives or substitutes of ODS are currently evolved. New technology for phase out ODS is also designed. It is clear in Table 4.

Table 4. The ozone depleting substances (ODS) and currently evolving substitutes or alternatives used in sectors and subsectors in industry in India.

Sl. No.	Sector	Subsectors	Application	ODS	Currently evolving alternatives/substitutes
1.	Refrigeration and air conditioning	(a) Domestic Refrigerators	Initial charges Recharge	CFC-12(CCl_2F_2) CFC-12	HFC-134a, HFC-(CH_3CF_2H) and Blends, Hydrocarbons (propane/butane, propane/isobutane mixtures)
		(b) Central air conditioning plants	Initial charges Recharges	CFC-11/CFC-12 CFC-11 (CCl_2F)/CFC-12	HCFC-123/HFC-134a HCFC-123 (CCl_2HCF_4)/HFC-134a (CF_2CFH_4)
		(c) Ice candy machines	Initial charges Recharges	CFC-12 CFC-12	HCFC-22, HFC-143a ($CClF_2H$)
		(d) Refrigerated cabinets	Initial charges Recharges	CFC-12 CFC-12	HFC-134a, HFC-152a Mixtures and hydrocarbons
		(e) Mobile air-conditioning	Initial charges Recharges	CFC-12 CFC-12	HFC-134a mixtures
		(f) Others · Water cookers, Process chikers, cold stores, walk-in-coolers, room air-conditioners, shipping, etc.	Initial charges Recharges	CFC-12 CFC-12	HCFC-22, HFC-134a, HFC-152a Hydrocarbons and mixtures
2.	Foams	(a) Flexible PUF			
		(i) Slabstock	Mattress, furniture, padding	CFC-11	Methylene chloride
		(ii) Moulded	Automotive furniture	CFC-11	
		(b) Rigid PUF			
		(i) Refrigeration insulation	Domestic refrigerators, freezers	CFC-11	HCFC-22/HCFC-142b ($CH_4CCl_4F_2$), HFC-134a HCFC-141b (CH_3CCl_2F)
		(ii) General insulation	Cold storage, boilers, building	CFC-11	HCFC-123, HCFC-141b
		(iii) Thermo ware	Thermobottles, cassesoles	CFC-11	HCFC-22, HCFC-123
		(c) Thermoplastic foam polystyrene, polyolefine	Fast food packaging	CFC-11/CFC-12	HCFC-22, CO_2
		(d) Miscellaneous	Building, shoe industry, furniture, automotive packaging *etc.*	CFC-11/CFC-13 ($C_2Cl_3F_3$)	—
3.	Solvents	(a) Electronics and precision cleaning		(i) CFC-113	No clean technology (*e.g.* LS flux application, controlled atmosphere, soldering)
				(ii) CTC (CCl_4)	Aqueous cleaning

Table 4. *(Cont'd.)*.

Sl. No	Sector	Subsectors	Application	ODS	Currently evolving alternatives/substitutes
				(iii) MCF (CH_3CCl_3)	Cleaning process, organic non-halogenated solvents (*e g.* alcohol, ketones, glycols, esters, terpenes, petroleum distillators *etc.* along with compatible fluxes). Halogenated solvents (*e g* trichloroethylene, perchloroethane *etc.*), perfluoro carbon *e g* perchlorohexane) A combination of the above
		(b) Textile cleaning		CTC	Chlorinated solvents, hydrocarbons based solvents, aqueous systems and HCFCs
		(c) Pesticides and pharmaceutical		CTC	Process modification, chlorinated solvents, hydrocarbons and a combination of the former
		(d) Rubber industry		CTC	(i) New sealed system/recycling technology (zero emissions) (ii) New emerging technology to be identified
		(e) Coating		CFC-113 MCF	Aqueous solvents, Chlorinated solvents, perfluro carbons, controlled mechanical applications
		(f) Chemicals and laboratory		CTC	Aqueous solvents, organic non-halogenated solvents
4	Aerosols	Personal products : Perfumes sprays, shaving foam, industrial aerosols, silicone sprays, mould release, house hold products, room freshners, insecticides, automotive products, paints, tyre, inflators, pharmaceutical products		CFC-11 and CFC-12	Hydrocarbon aerosol, propellant (blends of destenched, LPG, propane and n-Butane), dimethyl ether
5	Fire extinguishing	Fire extinguishing Fire extinguishing	Portable (partly fixed) fixed system	Halone-1211 Halone-1301	ABC powder, foams, CO_2, inert gases, water fog/mist, fast response sprinklers etc.

The estimation for the production excluding exports and reduction of ODS consumption for the period 1996-2010 is also clear from Figure 12. In the Figure 13, the requirements of important ODS substitutes for the said period is also estimated.

Major industrial nations signed up to rules and agreements taken at the United Nations Climate Change Conference in Kyoto on 1–11 December, 1997 on limiting green house gas emissions. According to the third Conference of the Parties to the UN Frame work Convention on climate Change (COP-3), the overall targets adopted for green house gas emissions by 2008–12 are an 8% cut from 1990 levels for the European Union (EU), 7% for the USA, 6% for Japan and Canada, Australia is allowed an 8% increase, while Russia has a target of 0%. Compared with the oppeaning position of 15% for the EU, 5% for Japan, and 0% for the

USA, this seems like a tidy compromise. According to COP-4, 1998, the case of nuclear power must now be considered. According to WWF, the current agreement

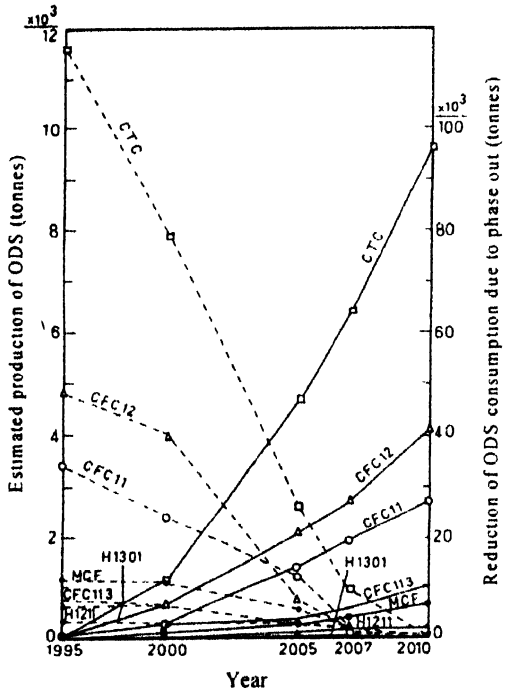

Figure 12. Estimated production of ODS and reduction of ODS consumption due to phase out for the year 1996–2010 in India.

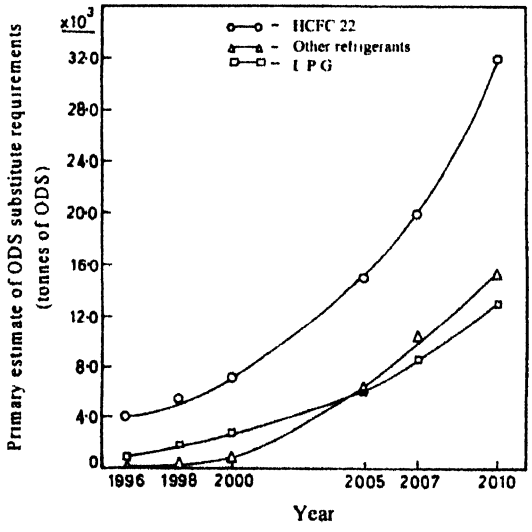

Figure 13. Primary estimate of ODS substitute requirements for the year 1996–2010 in India

will achieve a 2% cut in green house gas emissions by 2010, rather than the 5% predicted under the original protocol [318].

Acknowledgment

The authors wish to thank D Midya for supplying the ozone data from Internet system. The authors wish to thank Government of India for publishing "Country Programme, Phase out of Ozone Depleting Substances under the Montreal Protocol" in September 1993. From this publication, the data of ODS and its substitutes or alternatives are collected.

References

[1] J C Farman, B G Gardiner and J D Shanklin *Nature* **315** 207 (1985)

[2] C R Sreedharan, G S Rao and P M Gulhane *Indian J. Radio Space Phys* **18** 188 (1989)

[3] A F G Jacobs and H Hakvoort *Kema Sci Tech Rep.* **8** 401 (1990)

[4] K A Cavender and E R Allen *Proc-A & WMA Annl Meet* 5 90/955 16 (1990)

[5] L S Pardede *Ozone Depletion, 1990* (ed) Ilyas Mohammad (Univ Sci., Malaysia) p 189 (1991)

[6] W D Komhyr, R D Evans, R D Grass, G L Koenig and J A Lathrop *Report 1990* NOAA-DR-ERL-CMDL-6 23 (1990)

[7] T S McDermid, S M Godin and T D Walsh *Appl. Opt.* **29** 4914 (1990)

[8] J L Bertaux, G Megie, T Widemann, E Chassefiere, R Pellinen, E Kyrola, S Korpala and P Simon *Adv Space Res* **11** 237 (1991)

[9] M Derek and E R Veiga *Adv Space Res.* **11** 5 (1991)

[10] H Hankola, S Joffre, H Lattila and P Taalas *Atmos Environ Part A* **25** 1437 (1991)

[11] D W Fahey *Proc. PIE-Int Soc Opt. Engg.* **1433** 212 (1991)

[12] U Schurath, W Speuser and R A Schmidt *J. Anal Chem* **340** 544 (1991)

[13] M Luisa and M J G Sanz *J. An Fis Ser B* **87** 101 (1991)

[14] H Oelhaf, T Vonclarmann, F Freg, H Fisher, F Friedle-Vallone C Fritzsche, C Piesch, D Rabus, M Seefeldner and M Voelker *Euro. Space Agency (Sp Publ.)* ES ASP 1991 ESASP-317 207 (1991)

[15] J H Duyzer *Precip Scavenging Atmos-Surf Exch* [Proc 5th Int Conf 1991] **2** p 1105 (eds) S E Schwartz, W Slinn and G N Hemisphere (Washington DC) (1992)

[16] C Pilinis and S Marsh *Proc 84th Annl Meet. Air Waste Manage Assoc 1991* (Vol. 5) Paper 91/66.1 p 16 (1991)

[17] A Matsuzaki *Anal Sci* 7 1021 (1991)

[18] W D Komhyr, J Wendell and J A Lathrop *Report 1991* NOAA-DR-ERL-CMDL-7 162 (1991)

[19] A E Roche and J E Kumer *Proc SPIE-Int. Soc. Opt Engg* **1491** 91 (1991)

[20] E V Browell *Proc SPIE-Int. Soc. Opt. Engg.* **1491** 7 (1991)

[21] D J Hofmann and T Deshler *Nature* **349** 300 (1991)

[22] M Zunckel, M W J Scourfield and R D Diab *S. African J Sci* **88** 217 (1992)

[23] S Chen, D Chen and X Tang *Huanjing Huaxue* **11** 14 (1992)

[24] B Gomiscek and H Puxbaum *Vestn Slov Kem Drus* **39** 9 (1992)

[25] P Taalas and E Kyro *J. Atmos. Terr. Phys.* **54** 1089 (1992)

[26] X Niu, J E Frederick, M L Stein and G E Tiao *J. Geophys. Res. (Atmos.)* **97D** 14661 (1992)

[27] Y J Kaufman, A Setzer, D Ward, D Tancre, B N Holben, P Menzel, M C Pereira and R Rasmussen *J. Geophys Res* **97D** 14581 (1992)

[28] E Varotsos *Bilateral Seminar Int. Bur.* (Seminar on Monitoring and Modelling in the Mesoscale) 95 (1992)

[29] E E Uthe, J M Livingston and N B Nielsen *J. Air Waste Manage Assoc.* **42** 1313 (1992)

[30] D DeMuer and H DeBacker *J. Geophys. Res.* **97D** 5921 (1992)

[31] A V Kal'sin, V N Lebedinets, N V Tereb, D A Andrienko, L M Belokrinitskaya, A V Belyavsky, V N Vashchenko, V A Danilevskii and A A Zhitetskii *Adv. Space Res.* **13** 329 (1993)

[32] H K Roscoe, R L Jones, R A Freshwater, D J Fish, R Wolfenden, J E Harries and D J Oldham *Pro. SPIE-Int. Soc. Opt. Engg.* **1715** 374 (1993)

[33] J J Barnett, P E Morris, T J Nightingale, E W P Palmer, G D Peskett, C D Rodgers, F W Taylor, P Venters and R J Wells *Proc. SPIE-Int. Soc. Opt. Engg.* **1715** 527 (1993)

[34] R McPeters *Proc. SPIE-Int. Soc. Opt. Engg.* **1715** 522 (1993)

[35] A C Vandaele, M Cerler, R Colin and P C Simon *Proc SPIE-Int. Soc. Opt. Engg.* **1715** 288 (1993)

[36] R D Boime and S G Warren *Proc.-Int. Soc. Opt. Engg.* **2047** 122 (1993)

[37] A Theodorsen, S Bersas, H Oernes, K Henriksen and A Vasilive *Proc SPIE-Int. Soc. Opt. Engg.* **2047** 180 (1993)

[38] V L Larin, M I Beloglazov, L L Lazutin, S A Rumyantsev and A N Vasilev *Proc. SPIE-Int. Soc. Opt. Engg.* **2047** 207 (1993)

[39] P Domnin *Proc. SPIE-Int. Soc. Opt. Engg.* **2047** 242 (1993)

[40] D DeMuer and H DeBarker *Proc. SPIE-Int. Soc. Opt. Engg.* **2047** 18 (1993)

[41] J W Waters, L Froidevaux, N G Read, G L Manney, L S Elson, D A Flower, R F Jarnot and R S Harwood *Nature* **362** 579 (1993)

[42] E V Browell, M A Fenn, C F Butler, W B Grant, R C Harriss and M C Shiplam *J Geophys Res.* **99** 1739 (1994)

[43] G M Keating, L S Chiou and N C Hsu *Adv Space Res.* **14** 201 (1994)

[44] D Kley, P J Crutzen, H G J Smit, H Vomel, S J Oltmans, H Grassl and V Ramanathan *Science* **274** 230 (1996)

[45] M E Summers, R R Conway, D E Siskind, M N Stevens, D Offermann, M Riese, P Preusse, D F Strobel and J M Russell III *Science* **277** 1967 (1997)

[46] H K Roscoe, A E Jones and A M Lee *Science* **278** 93 (1997)

[47] A E Waibel, T Peter, K S Carslaw, M Oelhaf, G Wetzel, P J Crutzen, U Poschl, A Tsias, E Reimer and H Fisher *Science* **283** 2064 (1999)

[48] D J Hofmann, J W Harder, S R Rolf and J M Rosen *Nature* **326** 59 (1986)

[49] M R Schoeberl and A J Kruger *Geophys. Res. Lett.* **13** 1191 (1986)

[50] Y Iwasaka *Geophys. Res. Lett.* **14** 87 (1987)

[51] A C Aikin and R D McPeters *Geophys. Res. Lett.* **15** 413 (1988)

[52] B G Gardiner *Geophys. Res. Lett.* **15** 901 (1988)

[53] R T Watson *Ozone Trends Panel, Present State of Knowledge of the Upper Atmosphere, 1988, An Assessment Report, (NASA)* (Ref. Publ. 1208, NASA, Washington DC) (1989)

[54] R C Schnell, S C Liu, S J Oltmans, R S Stone, D J Hofmann, E G Dutton, T Deshler, W T Struges, J W Harder, S D Sewell, M Trainer and J M Narris *Nature* **351** 726 (1991)

[55] J Austin, N Butchart and K P Shine *Nature* **360** 221 (1992)

[56] S Bekki, R Toumi and J A Pyle *Nature* **362** 331 (1993)

[57] R J Salawitch, S C Wofsy, E W Gottlieb, L R Lait, P A Newman, M R Schoeberl, M Loewenstein, J R Podolske, S E Strahan, M H Proffit, C R Webster, R D May, D W Fahey, D Baumgarcher, J E Dye, J C Willson, K K Velly, J W Elkins, K R Chen and J G Anderson *Science* **261** 1146 (1993)

[58] M H Proffitt, K Aikin, J J Margitan, M Loewenstein, J R Podolske, A Weaver, K R Chen, H Fast and J W Elkins *Science* **216** 1150 (1993)

[59] G Walker *Nature* **365** 683 (1993)

[60] F Froidevaux *J. Atmos. Sci.* **51** 2846 (1994)

[61] M L Santee *Science* **267** 849 (1995)

[62] D J Hofmann *Nature* **383** 129 (1996)

[63] B Navjokat and S Powson *Geophys. Res. Lett.* **23** 3703 (1996)

[64] R W Zurek *Geophys Res. Lett.* **23** 289 (1996)

[65] L Coy *Geophys Res Lett.* **24** 2693 (1997)

[66] P Aldhous *Nature* **404** 531 (2000)

[67] S N Ghosh and S K Midya *Indian J. Phys.* **68B** 473 (1994)

[68] S Chapman *Mem. Roy. Met. Soc.* **3** 103 (1930)

[69] B J F Pitts and J N Pitts (Jr) *Science* **276** 1045 (1997)

[70] W L Chameides and J C G Walker *J. Geophys. Res.* **78** 8751 (1973)

[71] P J Crutzen *Pure Appl. Geophys* **1385** 106 (1973)

[72] A K Attri, U Kumar and V K Jain *Nature* **411** 1015 (2001)

[73] J G Slanger, L E Jusinski, G Black and G E Gadd *Science* **241** 945 (1988)

[74] G I Gellene *Science* **274** 1344 (1996)

[75] D Krankowsky *Geophys. Res. Lett.* **22** 1713 (1995)

[76] D Krankowsky and K Mauersberger *Science* **274** 1324 (1996)

[77] J C Johnston and M H Thiemens *J. Geophys. Res.* **102** 25395 (1997)

[78] F W Iron *Geophys. Res. Lett.* **23** 2377 (1996)

[79] M H Thiemens and T Jackson *Geophys. Res. Lett.* **15** 639 (1988)

[80] M H Thiemens and T Jackson *Geophys Res. Lett.* **17** 717 (1990)

[81] J Morten, J Barnes, B Schueler and K Mauersberger *J. Geophys. Res.* **95** 901 (1990)

[82] K Mauersberger, B Erbachar, D Krankowsky, J Gunther and R Nickel *Science* **283** 370 (1999)

[83] S M Anderson, D Hulsebusch and K Mauersberger *J. Chem. Phys.* **107** 5385 (1997)

[84] M H Thiemens *Science* **293** 226 (2001)

[85] P J Crutzen and U Schmailzl *Planet Space Sci.* **31** 1009 (1983)

[86] S Bekki and J A Pyle *J. Geophys. Res.* **97** 15839 (1992)

[87] H Okabe *Photochemistry of Small Molecules* (New York : Willey-Interscience) (1978)

[88] H Levy II *Planet Space Sci.* **20** 919 (1972)

[89] A M Thompson *Science* **256** 1157 (1992)

[90] G P Ayers, S A Penkett, R W Gillett, B Bandy, I E Galbally, C P Meyer, C M Elsworth, S T Bently and B W Forgan *Nature* **360** 446 (1992)

[91] M J Molina and F S Rowland *Nature* **249** 810 (1974)

[92] L T Molina and M J Molina *J. Phys. Chem.* **91** 433 (1987)

[93] S C Wofsy, M B McElroy and Y L Yung *Geophys. Res. Lett.* **2** 215 (1975)

[94] J C McConnel *Nature* **355** 150 (1992)

[95] S M Fan and J J Daniel *Nature* **359** 522 (1992)

[96] M Eigen and K J Kustin *J Am. Chem. Soc.* **84** 1355 (1962)

[97] M B McElroy, R J Salawitch, S C Wofsy and J S Logan *Nature* **321** 759 (1986)

[98] W H Brune, J G Anderson, D W Toohey, D W Fahey, S R Kawa, R L Jones, D S McKenna and L R Poole *Science* **252** 1260 (1991)

[99] S Solomon, R R Garcia, F S Rowland and D J Wuebbles *Nature* **321** 755 (1986)

[100] J G Anderson, D W Toohey and W H Brune *Science* **251** 39 (1991)

[101] M O Andreae and P J Crutzen *Science* **276** 1052 (1997)

[102] S Bekki, R Toumi, J A Pyle and A E Jones *Nature* **354** 193 (1991)

[103] H S Johnston, D E Kinnison and D J Wuebbles *J. Geophys. Res.* **94** 16351 (1989)

[104] J A Anderson in *Research Summery 1994-1996 (NASA Upper Atmosphere Research Programme Report to Congress and the Environmental Protection Agency)* p 100 (1997)

[105] E C Zipf and S S Prasad *Science* **279** 211 (1998)

[106] M P McCormick and C R Trepte *J. Geophys. Res.* **92** 4297 (1987)

[107] D R Worsnop, L E Fox, M S Zahniser and S C Wofsy *Science* **259** 71 (1993)

[108] G Ritzhaupt and J P Devlin *J. Phys. Chem.* **95** 90 (1991)

[109] M A Tolbert and A M Middlebrook *J. Geophys. Res.* **95** 22423 (1990)

[110] B G Koehler *J. Geophys. Res.* **97** 8065 (1992)

[111] S Solomon *Rev. Geophys.* **26** 131 (1988)

[112] O B Toon, B P Hamill, R P Turco and J Pinto *Geophys. Res. Lett.* **13** 1284 (1986)

[113] D W Fahey *J. Geophys. Res.* **94** 11299 (1989)

[114] M P McCormick, H M Steele, P Hamill, W P Chu and T J Swissler *J. Atmos. Sci.* **39** 1387 (1982)

[115] P J Crutzen and F Arnold *Nature* **324** 651 (1986)

[116] M J Molina, T L Tso, L T Molina and F C Y Wang *Science* **238** 1253 (1987)

[117] M A Tolbert, M J Rossi, R Malhotra and D M Golden *Science* **238** 1258 (1987)

[118] S B Moore, L F Keyser, M T Leu, R P Turco and R H Smith *Nature* **345** 333 (1990)

[119] D R Hansen and A R Ravishankara *J. Geophys. Res.* **96** 17307 (1991)

[120] J P D Abbatt *J. Geophys. Res.* **97** 15819 (1992)

[121] G M B Dobson, D N Harrison and J Lawrence *Proc. Roy. Soc. (London) Ser A* **129** 411 (1930)

[122] M W Chiplonkar *Proc Indian Acad. Sci. Sec. A* **10** 105 (1939)

[123] A Mani *Indian J. Radio Space Phys.* **19** 542 (1990)

[124] R V Karandikar and K R Ramanathan *Proc Indian Acad. Sci. Sec A* **29** 330 (1949)

[125] K R Ramanathan and K R Karandikar *Transactions IUGG Meeting held at Oslo in 1948, IATME Bulletion* **No.13** Part V p 492 (1950)

[126] K R Ramanathan and R N Kulkarni *Indian Acad. Sci. Sec. A* 37 321 (1953)

[127] K R Ramanathan *Presidential address in Scientific Proceedings of the International Association of Meteorology, IUGG 10th General Assembly held in Rome in 1954* (London : Butterworths) **3** (1956)

[128] K R Ramanathan and R N Kulkarni *QJR Meteorol. Soc.* **86** 144 (1960)

[129] K R Ramanathan *Indian J Meteorol Geophys.* **12** 391 (1961)

[130] K R Ramanathan *QJR Meteorol Soc. (GB)* **89** 540 (1963)

[131] K R Ramanathan *Annals of the IGY* (London : Pergamon) 32 p 101 (1964)

[132] K R Ramanathan *Presidential address in Proceedings of the Ozone Symposium held in 1964 at Albuquerque, World Meteorological Organization, Geneva* 1 (1965)

[133] C R Sreedharan *J Phys* E2 195 (1968)

[134] C R Sreedharan *PhD Thesis* (Kerala University, India) (1975)

[135] C R Sreedharan and V S Tewari *J Phys.* E4 706 (1971)

[136] B H Subbaraya and S Lal *Proc. Indian Acad Sci Earth Planet Sci.* **90** 173 (1984)

[137] B H Subbaraya *Proceedings of Indo-US Workshop on Global Ozone Problems held in 1983 at National Physical Laboratory* (New Delhi) (1984)

[138] B H Subbaraya, A Jayaraman and S Lal *Atmospheric Ozone* (eds) C S Zerefos and A Ghazi (Dordrecht, Holland : D Reidel) p 295 (1985)

[139] B H Subbaraya *Indian J Radio Space Phys.* **16** 25 (1987)

[140] B H Subbaraya, A Jayaraman, Y B Acharya, P Fabian, R Borchers and S Lal *Indian J Radio Space Phys.* **15** 67 (1986)

[141] M Vivekananda and R S Arora *Curr. Sci.* (India) **57** 1103 (1988)

[142] A P Mitra at *The Second Workshop on IMAP Results held at Trivandrum in 1988* (Indian Space Research Organization Bangalore) 1 (1989)

[143] Y V Somayajulu, K S Zalpuri and S Sampath *Indian J. Radio Space Phys.* **10** 197 (1981)

[144] S L Jain *IMAP Scientific Results ISRO-IMAP-SR-3288* (Indian Space research Organization, Bangalore) 202 (1988)

[145] C R Sreedharan, A N Chopra and A K Sharma *Indian J. Radio Space Phys.* **15** 159 (1986)

[146] C R Sreedharan, B K Hazra and R K Kankane *Proceedings of the International Symposium on Ozone held at Dresden in* (1976)

[147] A Jayaraman *PhD Thesis* (Gujarat University, India) (1985)

[148] S Lal, B H Subbaraya, R Borchors and P Fabian *IMAP Scientific Results ISRO-IMAP-SR-2188* (Indian Space Research Organization, Bangalore) 182 (1988)

[149] J Pandey, M Agrawal, N Khanan, D Narayan and D N Rao *Atmos Environ.* **26B** 91 (1992)

[150] C K Varshney and M Aggarwal *Atoms. Environ.* **26B** 91 (1991)

[151] C K Varshney and M Aggarwal *Environ. Monit. Assess.* **25** 41 (1993)

[152] B N Srivastava, M C Sharma and R S Tanwar *Indian J. Radio Space Phys.* **18** 296 (1989)

[153] G M Kumar, V Muralidharan, V N Neelakandan and S Sampath *Indian J. Radio Space Phys.* **18** 303 (1989)

[154] D K Chakrabarty and S K Peshin *J. Geophys. Res.* **102** 6153 (1997)

[155] D K Chakrabarty, S K Peshin, K V Pandya and N C Shah *J. Geophys. Res.* **103** 19245 (1998)

[156] P K Jana, S K Midya and U K De *Indian J Radio Space Phys.* **30** 176 (2001)

[157] V Ramanathan *Science* **190** 50 (1975)

[158] W C Wang *Science* **194** 685 (1976)

[159] V Ramanathan, R S Cicerone, H B Sing and J T Kiehl *J. Geophys. Res.* **90** 5547 (1985)

[160] W C Wang, M P Dudek, X Z Liang and J T Kiehl *Nature* **350** 573 (1991)

[161] J T Houghton (eds) *Intergovernmental Panel on Climate Change (IPCC), Climate Change 1995 The Science of Climate Change* (Cambridge : Cambridge Univ. Press) (1995)

[162] R N Harris and D S Chapman *Science* **275** 1618 (1997)

[163] H V Storch *Nature* **407** 449 (2000)

[164] S Huang, H N Pollack and P Y Shen *Nature* **403** 756 (2000)

[165] P D Jones, M New, D E Parker, S Martin and I G Rigor *Rev. Geophys.* **37** 173 (1999)

[166] P D Jones *Clim.* 7 1794 (1994)

[167] C Macilwain *Nature* **403** 233 (2000)

[168] H Rohde *Science* **248** 1217 (1990)

[169] A F Bouman in *Soils and the Green House Effect* (Chichesfer : Wiley) (1990)

[170] Levenberger and Siegenthaler *Nature* **360** 449 (1992)

[171] G T Haughton, J T Jenkins and J J Ephrams *Intergovernmental Panel on Climate Change (IPCC), Climate Change, the IPCC Scientific Assessment* (Cambridge : Cambridge Univ. Press) (1990)

[172] R A Kerr *Science* **282** 391 (1998)

[173] V Ramaswamy, M D Schwarzkopf and W Z Randel *Nature* **382** 616 (1996)

[174] R D Bojkov *WMO Bulletin* **41** 171 (1992)

[175] O B Toon, R P Turco and P Hamil *Geophys. Res. Lett.* **17** 445 (1990)

[176] S C Wofsy, R J Salawitch, J H Yalteau and M E McElroy *Geophys. Res. Lett.* **17** 449 (1990)

[177] M R Schoeberl and D L Hartmann *Science* **251** 46 (1991)

[178] R L Mckenzie *Global Ozone Reserch and Monitoring Project WMO Rep 37 Chap 9* (WMO Geneva) (1995)

[179] G Seckmeyer, B Mayer, G Bernhard, R L Mckenzie, P V Johnston, M Kotkamp, C R Booth, T Lucas and T Mestechikina *Geophys. Res. Lett.* **22** 1889 (1995)

[180] J E Frederick and A D Alberts *Gerphys. Res Lett.* **18** 1869 (1991)

[181] C R Booth, T Lucas, J H Morrow, C S Weiler and P A Penhale *The United States National Science Foundation's polar network for monitoring ultraviolet radiation, in* : C S Weiler and P A Penhale (eds). *Ultraviolet radiation in Antarctica, Measurements and Biological Effects, AGU Antarctic Research Series* **Vol. 62**, *American Geophysical Union* (Washington DC) **17** (1994)

[182] J E Fredrick, Z Qu and C R Booth *Photochem Photobiol* **68** 183 (1998)

[183] S Madronich, R L Mckenzie, L Ö Björn and M M Caldwell *J. Photochem Photobiol. B : Biology* **46** 5 (1998)

[184] J S Danial, S Solomon and D L Allritton *J. Geophys Res* **100** 1271 (1995)

[185] L K Bhutani *Indian J Radio Space Phys.* **18** 306 (1989)

[186] H Slaper, G J M Velders, J S Daniel, F R DeGruijl and J C Vanderleum *Nature* **384** 256 (1996)

[187] C D J Holman and B K Armstrong *J. Natl Canc. Inst.* **73** 75 (1984)

[188] J Scotto and T R Fears *Incidence in Non-melanoma Skin Cancer in the United States NIH Publication 82-2433* (National Institutes of Health, Washington DC) (1981)

[189] *Health Council of the Netherlands UV-Radiation from Sunlight the Hague 1994/05E* (Health Council of the Netherlands, the Haque) (1994)

[190] A M Hargis *Compendium Continuing Educ.* **3** 987 (1981)

[191] A Mendez, J Perez, E Rniz-Villamor, M P Martin and E Mozos *Veterinary Record* **141** 597 (1997)

[192] J P Teifke and C V Lohr *J. Compar. Pathol.* **114** 205 (1996)

[193] K E Kopecky, G W Pugh and D E Hughes *Am J. Veterinary Res.* **41** 1412 (1980)

[194] S J Mayer *Veterinary Record* **131** 120 (1992)

[195] J C Merriam *Trans. Am Ophthalmol. Soc.* **94** 804 (1996)

[196] C A McCarty and H R Taylor *Invest Ophthalmol. Visual Sci.* **37** 1720 (1996)

[197] F C Hollows *Trans Menzies Foundation* **15** 113 (1989)

[198] *Italian-American Cataract Study Group Am. J Epidemiol.* **133** 542 (1991)

[199] *Italian-American Cataract Study Group Am. J. Ophthalmol.* **188** 623 (1994)

[200] *Scientific Assessment of Ozone Depletion : 1994* in D L Albritton, R T Watson and P J Aucamp (eds) *Global Ozone Research and Monitoring Project Report No 37* (World Meteorological Organization, Geneva) (1994)

[201] C Brühl and P J Crutzen *Geophys. Res. Lett.* **16** 103 (1989)

[202] S Madronich, L O Björn, M Ilyas and M M Caldwell *Changes in biologically active ultraviolet radiation reaching the earth's surface* in : J C VanderLeun, M Tevini, R C Worrest (eds). *Environmental Effects of Ozone Depletion 1991 Update, United Nations Environment Programme, Nairobi* (1991)

[203] J E Fredrick, A E Koob, A D Alberts and E C Weatherhead *J. Appl. Meteorol.* **32** 1883 (1993)

[204] M Blumthaler, W Ambach and R Ellinger *J. Photochem. Photobiol. B : Biol.* **39** 130 (1997)

[205] J Ma and R Guicherit *Photochem. Photobiol.* **66** 346 (1997)

[206] G Seemeyer and R L Mckenzie *Nature* **359** 135 (1992)

[207] J Fishman *Chemosphere* **22** 685 (1991)

[208] M Berry, P J Lioy, K Gelperin, G Buckler and J Kholtz *Environ Res.* **54** 135 (1991)

[209] D M Spector, G D Thurston, J Mao, D He, C Hayes and M Lippmann *Environ Res.* **55** 107 (1991)

[210] Y Chen, O Fang, K Wang and N Wang *Nanjing Yixueyuam Xuebo* **12** 276 (1992)

[211] R G Whitefield, T S Wallston, R L Winkler and H M Richmond *Report* (1991), ANL/EAIS-2, Order No. DE 91016814, 108 (1991)

[212] H OzKaynak, P L Kinney and B Burbank *Proc A & WMA 83nd Annual Meet* (1990) **Vol. 83** 90/150 6 11 (1990)

[213] R P Cody, C P Weisel, G Birnbaum and P J Lioy *Environ. Res.* **58** 184 (1992)

[214] W J Manning, J R Bergman and J T O' Brien *Proc. 84th Annual Meet-Air Waste Manage Assoc* **Vol. 15B** 91/144.5 9 (1991)

[215] T Naganuma, S Konishi, T Inove, T Nankane and S Sukizaki *Marine Ecol Progr Ser* **135** 309 (1996)

[216] R G Wetzel, P G Hatcher and T S Biandi *Limnol Oceanogr.* **40** 1369 (1995)

[217] R Pienitz and W F Vincent *Nature* **404** 484 (2000)

[218] D Karentz, M L Bothwell, R B Coffin, A Hanson, G J Herndl, S S Kilham, M P Lesser, M Lindell, R F Moeller, D P Morris, P J Neale, R W Sanders, C S Weiler and R G Wetzel *Archiv. fur Hydro Biologie Beiheft* **43** 31 (1994)

[219] F Garcia Pichel *Limnol Oceanogr.* **39** 1704 (1994)

[220] W H Jeffrey, P Aas, M MailleLyons, R B Coffin, R J Pledger and D L Mitchell *Photochem. Photobiol.* **64** 419 (1996)

[221] W H Jeffrey, R J Pledger, P Aas, S Hager, R B Coffin, R V Hauen and D L Mitchell *Diel Marine Ecol Progr Ser* **137** 283 (1996)

[222] G Muller Niklas, A Heissenberger, S Puskaric and G J Herndl *Aquat. Microbial Ecol.* **9** 111 (1995)

[223] P Aas, M Lyons, R Pledger, D L Mitchell and W H Jeffrey *Aquat Microbial Ecol.* **11** 229 (1996)

[224] R Sommaruga, M Krössbacher, W Salvenmoser, J Catalan and R Psenner *Aquat. Microbiol.* **9** 305 (1995)

[225] R Sommaruga, A Oberleiter and R Psenner *Appl Enviornment. Microbiol* **62** 4395 (1996)

[226] A K Kashyap, K D Pandey and R K Gupta *Folia Microbiologica* **36** 557 (1991)

[227] R P Sinha, N Singh, A Kumar, H D Kumar, M Hader and D P Häder *J Photochem. Photobiol B : Biol.* **32** 107 (1996)

[228] R P Sinha and D P Häder *Photochem. Photobiol* **64** 887 (1996)

[229] A Kumar, M B Tayagi, G Srinivas, N Sign, H D Kumar, R P Sinha and D P Häder *Photochem. Photobiol.* **64** 321 (1996)

[230] V A Donkar and D P Häder *Aquat. Microbial Ecol.* **11** 143 (1996)

[231] V A Donkar and D P Häder *Acta Protozoologica* **36** 49 (1997)

[232] R P Sinha, H D Kumar, A Kumar and D P Häder *Acta Protozoologica* **34** 187 (1995)

[233] R Araoz and D P Häder *FEMS Microbiol. Ecol.* **23** 301 (1997)

[234] A Kumar, R P Sinha and D P Häder *J. Plant Physiol.* **148** 86 (1996)

[235] V A Donker and D P Häder *J. Plant Physiol.* **145** 750 (1995)

[236] U Karsten and F Garcia Pichel *Appl. Microbiol.* **19** 285 (1996)

[237] I R Vassiliev, O Prasil, K D Wyman, Z K Kolber, A K Hanson, J E Prentiv and P G Falkowski *Photosynth Res.* **42** 51 (1994)

[238] H Herrmann, D P Häder, M Köfferlein, H K Seidlitz and F Ghetti *Med. Biol. Environ.* **23** 36 (1995)

[239] H Herrmann, D P Häder, M Köfferlein, H K Seidlitz and F Ghetti *J Photochem. Photobiol. B Biol.* **34** 21 (1996)

[240] H Herrmann, D P Häder and F Ghetti *Plant Cell Environ.* **20** 359 (1997)

[241] G M Giacomelti, R Barbato, S Chiaramonte, G Friso and F Rigoni *Eur. J. Biochem* **242** 799 (1996)

[242] F L Figueroa, C Jimenez, L M Lubian, O Montero, M Lebert and D P Häder *J. Plant Physol* **151** 6 (1997)

[243] W W C Gieskes and A G J Buma *Plant Ecology* **128** 16 (1997)

[244] S Gerber and D P Hader *FEMS Microbiol. Ecol.* **16** 33 (1995)

[245] S Gerber and D P Häder *Acta Protozoologica* **34** 132 (1995)

[246] A G J Buma, H J Zemmelink, K Sjollema and W W C Gieskes *Marine Ecol Progr Ser* **147** 47 (1996)

[247] H Peletier, W W C Gieskes and A G J Buma *Marine Ecol. Progr Ser* **135** 163 (1996)

[248] M J Behrenfeld *J Physiol* **31** 25 (1995)

[249] G Döhler *Botanica Acta* **109** 35 (1996)

[250] G Döhler *J. Plant Physiol.* **151** 550 (1997)

[251] G Döhler and E Hagmeier *Botanica Acta* **110** 481 (1997)

[252] G Döhler, E Hagmeier and C David *J. Photochem. Photobiol B Biol.* **30** 179 (1995)

[253] R Scheverlein, S Treml, B Thar, U K Tirlapur and D P Häder *J Photochem photobiol B Biol* **31** 113 (1995)

[254] A G J Buma, E J VanHannen, L Roza, M J W Veldhuis and W W C Gieskes *J Phycol* **51** 314 (1995)

[255] A G J Buma, E J VanHannen, L Roza, M J W Veldhuis and W W C Gieskes *UV-induces DNA damage and DNA synthesis delay in the marine diatom cyclolella sp; Scientia Marina 60* (Suppl. 1) (Barcelona, Spain) p 101 (1996)

[256] A G J Buma, A H Engelen and W W C Gieskes *Marine Ecol Progr Ser* **153** 91 (1997)

[257] K Banse *J Marine Sci.* **52** 265 (1995)

[258] K Roemmich and J McGowan *Science* **267** 1324 (1995)

[259] K D Malloy, M A Holman, D Mitchell and H W Detrich III *Proc Natl. Acad. Sci. (USA)* **94** 1258 (1997)

[260] T Naganuma, T Inoue and S Uye *J. Plankton Res.* **19** 783 (1997)

[261] L Chalker Scott *Marine Biol.* **123** 799 (1995)

[262] J M Shick, M Lesser and P L Jokiel *Global Change Biology* **2** 527 (1996)

[263] B E Brown, R P Dunne, T P Scoffin and M D A leTissier *Marine Ecol. Prog. Ser.* **105** 219 (1994)

[264] D F Gleason and G M Wellington *Marine Biol.* **123** 693 (1995)

[265] A K Caroll and J M Shick *Marine Biol.* **124** 561 (1996)

[266] J R Hunter, S E Kaupp and J H Taylor *Assessment of Effects of UV Radiation on Marine Fish Larvae in :* J Calkins (ed) *The Role of Solar Ultraviolet Radiation in Marine Ecosystems* (New York : Plenum) **459** (1982)

[267] E E Little and D L Fabacher *Archiv. für Hydrobiologie Beiheft* **43** 217 (1994)

[268] J H M Kouwenberg, H I Browman, J J Cullen, R F Davis, J F St Pierre and J A Runge *Marine Biol.* (1998)

[269] C E Williamsen, S L Metzger, P A Lovera and R E Moeller *Ecology Appl.* **7** 1017 (1997)

[270] R C Worrest and D J Kimeldorf *Photochem Photobiol.* **24** 377 (1976)

[271] J S Fuglestvedt, J E Jonson, W C Wang and I S A Isaksen *Responses in Tropospheric Chemistry to Changes in UV Fluxes, Temperatures and Water Vapour Densities* in : W C Wang and I S A Isaksen (eds.) : *Atmospheric Ozone as a Climate Gas, NATO ASI Series* **Vol. 132** (Berlin : Springer) p 145 (1995)

[272] J Ma *Effects of Clouds, Stratospheric Ozone Depletion and Tropospheric Pollution on the Chemical Budget of Ozone in the Troposphere through Changes in Photolysis Rates. TNO Institute of Environmental Science Report R 96/406, the Netherlands* (1996)

[273] R G Prinn, R F Weiss, B R Miller, J Huang, F N Alyea, D M Cunnold, P J Fraser, D E Hartley and P G Simmonds *Science* **269** 187 (1995)

[274] M Krol, P J Vanleeuwen and J Lelieveld *J Geophys. Res* **103** 10697 (1998)

[275] X Tang, S Madronich, T Wallington and D Calamari *J Photochem Photobiol B : Biol.* **45** 83 (1998)

[276] D M Etheridge, L P Steele, R J Francey and R L Langenfelds *J Geophys Res.* **103** 15979 (1998)

[277] R Zander, P Demoulin, D Ehhatt, U Scmidt and C Rinsland *J Geophys. Res.* **94** 11021 (1989)

[278] E Brunke, H Scheel and W Seiler *Atmospheric Environment* **24A** 585 (1990)

[279] P C Novelli, K A Masarie and P M Lang *Science* **263** 1580 (1994)

[280] C Granier, J F Müller, S Madronich and G P Brasseur *Atmos. Environ* **30** 1673 (1996)

[281] E J Dlugokencky, E G Dutton, P C Novelli, P P Tans, K A Masarie, K O Lantz and S Madronich *Geophys Res. Lett.* **23** 2761 (1996)

[282] A Sigg and A Neftel *Nature* **351** 557 (1991)

[283] M Anklin and R C Bales *J. Geophys. Res.* **102** 19099 (1997)

[284] A Neftel, R C Bales and D J Jacob *NATO ASI Series* **Vol. 130** (Berlin : Springer) 249 (1995)

[285] A L Andrady, S H Hamid, X Hu and A Torikai *J. Photochem Photobiol. B : Biology* **46** 96 (1998).

[286] N P Boucher and B B Prezelin *Marine Ecol. Progr. Ser.* **114** 223 (1996)

[287] P J Neale, R F Davis and J J Cullen *Nature* **392** 585 (1998)

[288] R C Smith, B B Prezelin, K S Baker, R R Bidigare, N P Boucher, T Coley, D Karents, S MacIntyre, H A Mallick, D Menzies, M Ondrusek, J Wan and K J Waters *Science* **255** 952 (1992)

[289] P J Neale, J J Cullen and R F Davis *Limonol Oceanogr.* **43** 433 (1998)

[290] A M Springer and C P McRoy *Continental Shelf Res.* **13** 575 (1993)

[291] C S Weiler and P A Penhale *Ultraviolet Radiation in Antarctica Measurements and Biological Effects* (American Geophysical Union : Washington DC) (1994)

[292] V Milot Roy and W F Vincent *Archiv Fur Hydrobiologie Beiheft* **43** (Special Isssue) 171 (1994)

[293] G Döhler *Marine Biol.* **112** 485 (1992)

[294] H Frank and A Klein *Nature* **382** 34 (1996)

[295] D Zehavi and J N Sciber *Anal Chem* **68** 3450 (1996)

[296] A Grimvall, H Boren, L vonSydow and K Laviewski *Analysis of TFA in Samples of Rain, Snow and Ice Collected at Remote Sites, Presentation to Alternative Fluorocarbons Environmental Assessment Study (AFEAS), US Geological Survey, Information Services* (Denver, CO) (1997)

[297] C E Wujcik, D Zehavi and J N Sciber *Chemosphere* **36** 1233 (1998)

[298] R S Thompson and A J Windeatt *Brixham Environmental Laboratory Report B L 5197/B* (1994)

[299] D Emerich *Effects of TFA on Symbiotic Nitrogen Fixation by Soybean, Final Report to Alternative Fluorocarbons Environmental Assessment Study (AFEAS), SP91-1824/BP 95 32* (University of Missouri) (US Geological Survey, Information Services, Denver, CO) (1997)

[300] A W Davison and S Pearson *Toxicity of TFA to Plants, Report to AFEAS, SP-91-1823/BP 96 31* (University of Newcastle) (US Geological Survey, Information Services, Denver, CO) (1997)

[301] R S Thompson *Brixham Environmental Laboratory Report BL 5474/B* (1995)

[302] R S Thompson, K M Stewart and E Gillings *Brixham Environmental Laboratory Report BL 5473/B* (1995)

[303] L S Kheilo and S N Kremneva *Gig Tr Prof Zabol* **10** 13 (1966)

[304] F A Patty *Industrial Hygiene and Toxiolgy* **Vol. II** 2nd Rev. Edn. in : *Toxicology* (New York . Inter Science) 1801 (1963)

[305] W W Just, K Gorgas, F U Hartl, P Heinemann, M Salzer and H Schimassek *Hepatology (Baltimore)* **9** 570 (1989)

[306] D B Warheit *Dupont Company, Haskell Laboratory Report HLR* 828-92 (1993)

[307] J Longstreth, F R deGruijl, M L Kripke, S Abseck, F Arnold, H I Slaper, G Velders, Y Takizawa and J C VanderLeun *J. Photochem. Photobiol. B : Biol.* **46** 20 (1998)

[308] S K Midya, P K Jana and T Lahiri *Earth, Moon and Planets* **66** 279 (1995)

[309] P K Jana and S K Midya *Earth, Moon and Planets* **75** 141 (1996)

[310] S K Midya, P K Jana and U K De *Indian J. Phys.* **73B** 605 (1999)

[311] S K Midya, S C Ganda and S N Sahu *Indian J. Phys.* **74B** 337 (2000)

[312] S K Midya, S C Ganda and S N Sahu *Mausam* **50** 403 (1999)

[313] S K Midya, S N Maitra and G Tarafdar *Indian J. Phys.* **75B** 15 (2001)

[314] S K Midya, S C Ganda and S N Sahu *Earth, Moon and Planets* **76** 5 (1997)

[315] S K Midya and D Midya *Earth, Moon and Planets* **61** 175 (1993)

[316] S N Maitra, S K Midya, G Tarafdar, B Bhattacharjee and S S Chatterjee *Asian J Microbiol Biotech Environ Sc* **2** 105 (2000)

[317] S K Midya, H Sarkar and A Manna *Czechoslovak J Phys* **51** 609 (2001)

[318] J Giles *Nature* **412** 365 (2001)

About the Reviewers

S K Midya

Dr. Subrata Kumar Midya obtained MSc (Physics) degree from Calcutta University in 1980 and PhD degree from Jadavpur University in 1988 on the basis of his thesis entitled, 'Airglow Emission and their Excitation Mechanisms'. His field of specialization is airglow, O_3 depletion and Interstellar Molecules. He has published 66 research papers in his fields of specialization in Indian and foreign journals. He is at present a Reader in Physics Department of Serampore College, Hooghly, West Bengal. In 2000, he was appointed as an honorary scientist for Centre for Space Physics, Kolkata, India.

P K Jana

Dr. Pratap Kumar Jana obtained MSc (Chemistry) degree from Calcutta University in 1988 and PhD Degree from Jadavpur University in 2001 on the basis of thesis entitled, 'Chemical Kinetics of Atmospheric Constituents and its Relation to Ozone Depletion'. He also carried out part time research works on Airglow emission and ozone depletion under guidance of Dr. S K Midya. He has published seven research papers and communicated three papers in different International Journals so far. He is at present an Asstt. Master of Howrah Zilla School, Office of the Headmaster, Govt. of West Bengal, India.